

# hp-VERSION ANALYSIS FOR ARBITRARILY SHAPED ELEMENTS ON THE BOUNDARY DISCONTINUOUS GALERKIN METHOD FOR STOKES SYSTEMS

EFTHYMIOS N. KARATZAS<sup>1</sup>

ABSTRACT. In the present work, we examine and analyze an alternative of the unfitted mesh finite element method improved by omitting computationally expensive, especially for fluids, stabilization type of penalty onto the boundary area, namely the so-called ghost penalty. This approach is based on the discontinuous Galerkin method, enriched by arbitrarily shaped boundary elements techniques. In this framework, we examine a stationary Stokes fluid system and we prove the inf/sup condition, the  $hp$ - a priori error estimates, to our knowledge for the first time in the literature, while we investigate the optimal convergence rates numerically. This approach recovers and integrates the flexibility and superiority of the unfitted methods whenever geometrical deformations are taking place, combined with the efficiency of the  $hp$ -version techniques based on arbitrarily shaped elements on the boundary.

## 1. INTRODUCTION

Recent years have shown scientists' interest significantly focused on the context of Galerkin finite element methods. This effort has given birth to new methods based on general-shaped elements which arise computational complexity reduction, like mimetic finite difference methods [9], virtual element methods [8], various discontinuous Galerkin approaches such as interior penalty Galerkin methods [15], and hybridized discontinuous Galerkin [17, 20], which are very attractive and used by the engineering and mathematics community. Other approaches have involved non-polynomial approximation spaces like polygonal and other generalized finite element methods, [28, 55]. In addition, various classes of fitted and unfitted mesh methods for interface or transmission problems may seen as generalized concepts of mesh elements, as well as, several unfitted finite element methods have been proposed in recent years, indicatively we mention the unfitted boundary finite element methods [5] and immersed finite element methods [42]. These approaches usually employ penalization on the boundary interface and/or weak enforcement of the boundary conditions and data usually supported by a level set geometry description, [49]. We refer to [15] for admissible polygonal/polyhedral element shapes for which the general interior penalty discontinuous Galerkin method (IP-dG), appears both stable and convergent while generalizes under mild assumptions the validity of standard approximation results, such as inverse estimates, best approximation estimates, and extension theorems.

In a  $p$ -version Galerkin framework achieving exponential convergence, for smooth PDE problems defined on general curved domains using isoparametrically mapped elements, we cite [47, 48], while for non-linear maps on element patches that are used to represent domain geometry we refer to [46, 53]. Although in both cases, as the polynomial order increases, the aforementioned mapping appears very costly and/or difficult to construct and implement in practice.

For Stokes flow systems, in [4, 56] an  $hp$ -discontinuous Galerkin approximation that shows better stability properties than the corresponding conforming ones is examined with finite element triangulation not required to be conforming employing discontinuous pressures and velocities, while it is defined on the interfaces between the elements involving the jumps of the velocity and the average of the pressure. The work of [30] also, describes a family of dG finite element methods formulated and analyzed for Stokes and Navier-Stokes problems introducing the good behavior of the inf-sup and optimal energy estimates for the velocity and pressure. In addition, this method can treat a finite number of nonoverlapping domains with nonmatching grids at interfaces.

In [18, 52], Stokes system local discontinuous Galerkin methods for a class of shape regular meshes with hanging nodes is investigated, as well as, several mixed discontinuous Galerkin approximations with their a priori error estimates.

---

<sup>1</sup>SCHOOL OF MATHEMATICS, ARISTOTLE UNIVERSITY OF THESSALONIKI, THESSALONIKI 54124, GREECE.

*E-mail address:* [ekaratz@math.auth.gr](mailto:ekaratz@math.auth.gr).

*Date:* January 31, 2023.

*Key words and phrases.* Arbitrarily shaped elements, discontinuous Galerkin finite element method,  $hp$ -version stability, a-priori estimates, fluid dynamics.

The early work of [51] handles the flow of a viscous incompressible fluid containing immersed boundaries which move with the fluid and exert forces on the fluid, and [58], a finite difference scheme with ghost cell technique is used to study viscous fluid flow with internal structures. In [50], a conservative cut-cell Immersed Boundary method with sub-cell resolution is analyzed.

For an immersed interface method for discrete surface representations employing accurate jump conditions evaluated along interface representations using projections, one could see [39], and for a ghost fluid method coupled with a volume of fluid method employing an exact Riemann solver [10]. For a fictitious domain finite element method, well suited for elliptic problems posed in a domain given by a level-set function without requiring a mesh fitting the boundary can be found in [25].

More extensively, an optimally convergent method of fictitious type domains avoiding the numerical integration on cut mesh elements for a Poisson system has been introduced in [41], while in [31] a method for the finite element solution of elliptic interface problem, using an approach due to Nitsche is proposed allowing discontinuities internal to the elements approximating the solution across the interface.

In addition, from a reduced basis for unfitted mesh methods point of view, evaluating the fixed background mesh used in immersed and unfitted mesh methods, parametrized Stokes and other flow systems have managed to be solved using a unified reduced basis presenting the flexibility of such methods in geometrically parametrized Stokes, Navier-Stokes, Cahn-Hilliard systems as in [34–38].

In [6], a new discontinuous Galerkin (DG) approach to simulations on complex-shaped domains, using trial and test functions defined on a structured grid with essential boundary conditions imposed weakly, where the discretization allows the number of unknowns to be independent of the complexity of the domain. [45] concerns an unfitted discontinuous Galerkin method proposing to discretize elliptic interface problems, where  $h$ - and  $hp$ - error estimates and convergence rates are proved. The authors of [57], treat an unfitted discontinuous Galerkin method for the elliptic interface problems, based on a variant of the local discontinuous Galerkin method, obtaining the optimal convergence for the exact solution in the energy norm and its flux in the  $L^2$  norm.

We extend the literature with [33], where a high-order hybridizable discontinuous Galerkin method for solving elliptic interface problems in which the solution and gradient are nonsmooth because of jump conditions across the interface and it is endowed with several distinct characteristics. [21] contains an unfitted mesh method for the Poisson interface problem constructing a novel ansatz function in the vicinity of the interface with an appropriate choice of flux for treating the jump conditions, designed through a delicate piecewise quadratic Hermite polynomial interpolation with a post-processing via a standard Lagrange polynomial interpolation.

In [7] an Unfitted Discontinuous Galerkin method for solving PDEs in complex domains, for transport processes in porous media problem is examined, allowing finite element meshes which are significantly coarser than those required by standard conforming finite element approaches. Further, in [27] an advection problem is developed based on an unfitted discontinuous Galerkin approach where the surface is not explicitly tracked by the mesh which means the method is flexible with respect to geometry efficiently capturing the advection driven by the evolution of the surface without the need for a space-time formulation, back-tracking trajectories or streamline diffusion. Finally, in [26] a linear transport equation on a cut cell mesh using the upwind discontinuous Galerkin method with piecewise linear polynomials and with a method of lines approach is presented employing explicit time stepping schemes, regardless of the presence of cut cells.

In the present work, we investigate the applicability of the interior-penalty discontinuous Galerkin method discretizing steady Stokes flow cases onto meshes with boundaries considering general, essentially arbitrarily shaped element shapes which allows attaining much smaller errors in coarser meshes. Furthermore, our analysis allows for curved element shapes, [13], without the use of any non-linear elemental maps. We use extensions of classical  $hp$ - trace and inverse estimates to arbitrary shape of boundary elements and we prove the inf-sup stability of the method in proper, to the prescribed method, norm. A priori error bounds for the resulting method are given under very weak assumptions restricting the magnitude of the local curvature of element boundaries on the boundary area. Numerical experiments are also presented, indicating the efficiency of the proposed framework.

The present work is structured as follows: we start with the Stokes flow model problem and the necessary preliminaries in Section 2. The various components of the interior penalty stabilized arbitrary boundary elements discontinuous Galerkin discretization are discussed in subsection 2.2 and we recall trace inverse estimates that are pivotal in the proof of the stability of IP-dG methods employed with the crucial independence of the element shape considering the constants that appear and affect several

inverse, stability and error estimates. Approximation results needed for the analysis of the method are collected in Section 3. Section 4 is devoted to stability estimates and the derivation of the discrete inf-sup condition, followed by a-priori error estimates in Section 5. Concluding, the aforementioned analysis is numerically verified with tests in Section 6 that depict the optimal theoretical  $hp$ -convergence rates and the  $hp$ -accuracy of the method.

It is noted that this work determines an approach where many expensive penalization terms can be omitted and appear beneficial especially, for fluid systems where additional penalization is needed. These results appear more relevant on the  $hp$ -version framework and geometries and verify that there is no loss of stability and accuracy, as traditionally appear e.g. in cases with excessive and/or insufficient penalization that typically results in accuracy loss. Further, we report that the theoretical tools presented are adapted on a Nitsche-type formulation of unfitted grid methods, and the a priori error analysis follows techniques of [14], [15]. The inf-sup stability result of the method in a Stokes like norm is proved on  $hp$ -approximation that will also lead to an error bound and optimal convergence rates. The theoretical developments presented regarding stability and a-priori error analysis of IP-dG methods, to the best of our knowledge are new for Stokes systems, and based on extensions of known inverse and trace inequalities, [16], allowing for more general curved element shapes see also [59] for an earlier, related result.

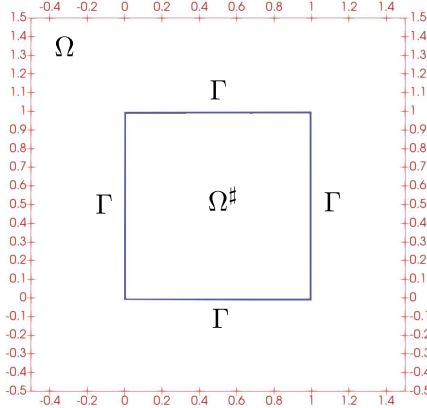


FIGURE 1. The geometry  $\Omega^\sharp$ , its boundary  $\Gamma$  and the auxiliary domain  $\Omega$ .

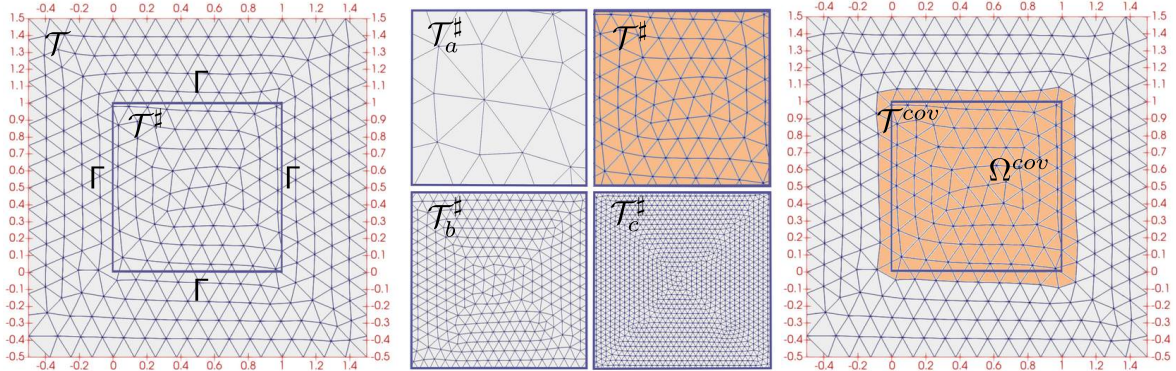


FIGURE 2. A mesh  $\mathcal{T}^\sharp$  based on arbitrarily-shaped boundary elements, the auxiliary background mesh  $\mathcal{T}$ , examples of refined  $\Omega^\sharp$  tessellations  $\mathcal{T}_a^\sharp$ ,  $\mathcal{T}_b^\sharp$ ,  $\mathcal{T}_c^\sharp$  and the covering domain/mesh,  $\Omega^{cov}/\mathcal{T}^{cov}$  respectively.

## 2. MODEL PROBLEM

**2.1. Problem formulation.** The steady Stokes equations for an incompressible viscous fluid confined in an open, bounded domain  $\Omega^\sharp \subset \mathbb{R}^d$  ( $d = 2, 3$ ) with Lipschitz boundary  $\Gamma = \partial\Omega^\sharp$  can be expressed

in the form

$$(2.1) \quad -\Delta \mathbf{u} + \nabla p = \mathbf{f} \text{ and } \nabla \cdot \mathbf{u} = 0 \quad \text{in } \Omega^\sharp, \quad \text{with } \mathbf{u} = 0 \quad \text{on } \Gamma.$$

Here  $\mathbf{u} = (u_1, \dots, u_d) : \Omega^\sharp \rightarrow \mathbb{R}^d$  ( $d = 2, 3$ ) and  $p : \Omega^\sharp \rightarrow \mathbb{R}$  denote the velocity and pressure fields, and  $\mathbf{f} \in [L^2(\Omega^\sharp)]^d$  is a forcing term. Since the pressure is determined by (2.1) up to an additive constant, we assume  $\int_{\Omega^\sharp} p dx = 0$  to uniquely determine  $p$ . Hence, in the following we will consider for pressure the standard space  $L_0^2(\Omega^\sharp) := \{q \in L^2(\Omega^\sharp) : \int_{\Omega^\sharp} q dx = 0\}$  of square-integrable functions with zero average over  $\Omega^\sharp$ .

Defining for all  $\mathbf{u}, \mathbf{v} \in V^\sharp := [H_0^1(\Omega^\sharp)]^d$  and  $p \in Q^\sharp := L_0^2(\Omega^\sharp)$  the bilinear forms

$$(2.2) \quad a(\mathbf{u}, \mathbf{v}) = \int_{\Omega^\sharp} \nabla \mathbf{u} : \nabla \mathbf{v} dx, \quad b(\mathbf{v}, p) = - \int_{\Omega^\sharp} p \nabla \cdot \mathbf{v} dx,$$

a weak solution to (2.1) is a pair  $(\mathbf{u}, p) \in [H_0^1(\Omega^\sharp)]^d \times L_0^2(\Omega^\sharp) = V^\sharp \times Q^\sharp$ , such that

$$(2.3) \quad A(\mathbf{u}, p; \mathbf{v}, q) = \int_{\Omega^\sharp} \mathbf{f} \cdot \mathbf{v} dx, \quad \text{for all test functions } (\mathbf{v}, q) \in V^\sharp \times Q^\sharp,$$

with

$$A(\mathbf{u}, p; \mathbf{v}, q) = a(\mathbf{u}, \mathbf{v}) + b(\mathbf{u}, q) + b(\mathbf{v}, p).$$

The well-posedness of (2.3) is standard [19].

**2.2. Arbitrarily shaped discontinuous Galerkin method on the boundary.** Implementation of an arbitrarily shaped boundary elements discontinuous Galerkin method for the discretization of (2.3) relies on a fixed auxiliary domain  $\Omega$  which contains the true geometry  $\Omega^\sharp$ , see Figure 1. Let  $\mathcal{T}$  be the corresponding auxiliary shape-regular mesh of  $\Omega$  and  $\mathcal{T}^\sharp$  is the mesh corresponding to  $\Omega^\sharp$ . The *active* mesh

$$\mathcal{T}^\sharp = \{K \cap \Omega^\sharp; \text{ for all } K \in \mathcal{T} \text{ with } K \cap \Omega^\sharp \neq \emptyset\}$$

is the minimal submesh of  $\mathcal{T}$  which covers  $\Omega^\sharp$  and is *fitted* to its boundary  $\Gamma$ : we allow mesh boundary elements  $K \in \mathcal{T}^\sharp$  which are arbitrarily-shaped and with very general interfaces. In the present work, numerical experiments consider boundary elements as Lipschitz curved elements and with only curved facet the one that coincides to the corresponding part of the boundary  $\Gamma$ , see Figures 1, 2 or the more general case of Figure 3. However, one could also employ general interfaces with neighboring elements, [15, 22, 24].

Finite element spaces for  $\mathbf{u}$  and  $p$  will be built upon the domain  $\Omega^\sharp = \bigcup_{K \in \mathcal{T}^\sharp} K$  which corresponds to  $\mathcal{T}^\sharp$ . The mesh skeleton  $\bigcup_{K \in \mathcal{T}^\sharp} \partial K$  –including the curved boundary facets– is subdivided into the internal part

$$\mathcal{F}_{int}^\sharp = \{F = K^+ \cap K^- : K^+, K^- \in \mathcal{T}^\sharp \text{ and } F \not\subseteq \Gamma\}$$

which actually denotes the set of interior faces in the active mesh, and the boundary part  $\Gamma \equiv \partial \Omega^\sharp$ . We denote by  $h_K = \text{diam}(K)$  the *local* mesh size for  $K \in \mathcal{T}^\sharp$  boundary elements and  $h_F = \min \{h_{K^+}, h_{K^-}\}$  for  $F = K^+ \cap K^-$ .

We choose to enforce boundary conditions at  $\Gamma$  to be weakly satisfied through Nitsche's method. We highlight that we do not employ coercivity recovery techniques applied over the whole computational domain  $\Omega$ , e.g. by means of additional ghost penalty terms which act on the gradient jumps –usually higher order– in the boundary zone; see, for instance, [11, 12, 34, 43]. Instead, the  $\mathcal{T}^\sharp$  coercivity is ensured following the approach of [15, 22].

To define the arbitrarily shape discontinuous Galerkin discretization for the Stokes problem (2.3), we employ the elementwise discontinuous polynomial finite elements for pressure and velocity spaces of order  $\mathfrak{p} \geq 1$ :

$$\begin{aligned} V_h^\sharp &\equiv S_{\mathcal{T}^\sharp, \mathbf{u}_h}^\mathfrak{p} := \left\{ w_h \in (L^2(\Omega^\sharp))^d : w_h|_K \in (\mathcal{P}^\mathfrak{p}(K))^d, K \in \mathcal{T}^\sharp \right\} \quad (d = 2, 3) \\ Q_h^\sharp &\equiv S_{\mathcal{T}^\sharp, p_h}^\mathfrak{p} := \{w_h \in L_0^2(\Omega^\sharp) : w_h|_K \in \mathcal{P}^{\mathfrak{p}-1}(K), K \in \mathcal{T}^\sharp\}. \end{aligned}$$

The broken Sobolev space  $H^s(\Omega, \mathcal{T}^\sharp)$ , with respect to the subdivision  $\mathcal{T}^\sharp$  up to composite order  $s$ , is defined as

$$H^s(\Omega^\sharp, \mathcal{T}^\sharp) = \{w \in L^2(\Omega^\sharp) : w|_K \in H^s(K) \ \forall K \in \mathcal{T}^\sharp\}.$$

It is important to mention that whenever the notation  $\nabla v$  is used for functions that lay in the discontinuous Galerkin space, i.e.  $w \notin H^1(\Omega^\sharp)$ , will correspond to the broken gradient, such that,  $(\nabla w)|_K = \nabla(w|_K)$  for all  $K \in \mathcal{T}^\sharp$ . So, the broken gradient  $\nabla_{\mathcal{T}^\sharp} w$  of a function  $w \in L^2(\Omega^\sharp)$  with  $w|_K \in H^1(K)$ , for all  $K \in \mathcal{T}$ , is defined element-wise by  $(\nabla_{\mathcal{T}^\sharp} w)|_K := \nabla(w|_K)$ . When  $F \subset \Gamma$ , it is

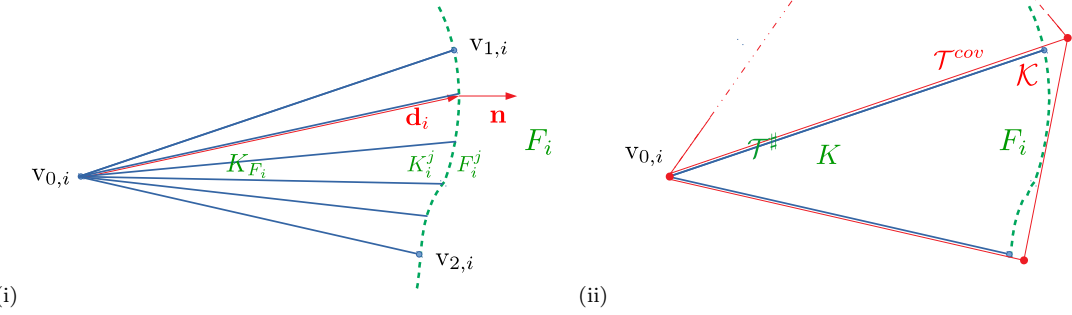


FIGURE 3. (i) Curved boundary elements for  $d = 2$  with one curved face and vertices  $\mathbf{v}_{k,i}$  and the unit outward normal vector to  $F_i$  at  $x \in F_i$  where  $K_{F_i}$  is star-shaped and (ii) the covering mesh  $\mathcal{T}^{cov}$ , and the mesh  $\mathcal{T}^{\#}$  corresponding to the truth geometry with arbitrary shape boundary elements.

$\{\{w\}\} = \llbracket w \rrbracket = w$  and  $\{\{\mathbf{w}\}\} = \llbracket \mathbf{w} \rrbracket = \mathbf{w}$ . The same applies for the broken divergence operator  $\nabla \cdot w$  defined element-wise. Moreover, recall the definition

$$\{\{w\}\} := \frac{1}{2} (w^+ + w^-), \quad \{\{\mathbf{w}\}\} := \frac{1}{2} (\mathbf{w}^+ + \mathbf{w}^-),$$

of the *average* operator  $\{\cdot\}$  across an interior face  $F$  for  $w$ ,  $\mathbf{w}$  scalar and vector-valued functions on  $\mathcal{T}^{\#}$  respectively, where  $w^{\pm}$  (resp.  $\mathbf{w}^{\pm}$ ) are the traces of  $w$  (resp.  $\mathbf{w}$ ) on  $F = K^+ \cap K^-$  from the interior of  $K^{\pm}$ . More precisely, with  $w^{\pm}(\mathbf{x}) = \lim_{t \rightarrow 0^+} w(\mathbf{x} \pm t\mathbf{n}_F)$  for  $\mathbf{x} \in F$  and  $\mathbf{n}_F$  we denote the outward-pointing unit normal vector to  $F$  and with  $\mathbf{n}_F$  the outward unit normal to the boundary  $\Gamma$ . The *jump* operator  $\llbracket \cdot \rrbracket$  across  $F$  is defined respectively by

$$\llbracket w \rrbracket := w^+ - w^-, \quad \llbracket \mathbf{w} \rrbracket := \mathbf{w}^+ - \mathbf{w}^-.$$

We are now ready to formulate a discrete counterpart of (2.3) through a discontinuous Galerkin method. The symmetric interior penalty discretizations of the diffusion term and the pressure–velocity coupling in (2.2) lead to the bilinear forms

$$\begin{aligned} a_h(\mathbf{u}_h, \mathbf{v}_h) &= \int_{\Omega^{\#}} \nabla \mathbf{u}_h : \nabla \mathbf{v}_h \, d\mathbf{x} - \sum_{F \in \mathcal{F}_{int}^{\#} \cup \Gamma} \int_F (\{\nabla \mathbf{u}_h\} \cdot \mathbf{n}_F \llbracket \mathbf{v}_h \rrbracket + \{\nabla \mathbf{v}_h\} \cdot \mathbf{n}_F \llbracket \mathbf{u}_h \rrbracket) \, d\gamma \\ &\quad - \int_{\Gamma} \mathbf{u}_h \nabla \mathbf{v}_h \cdot \mathbf{n}_{\Gamma} \, d\gamma - \int_{\Gamma} \mathbf{v}_h \nabla \mathbf{u}_h \cdot \mathbf{n}_{\Gamma} \, d\gamma + \int_{\Gamma} \sigma \mathbf{u}_h \mathbf{v}_h \, d\gamma + \sum_{F \in \mathcal{F}_{int}^{\#} \cup \Gamma} \int_F \sigma \llbracket \mathbf{u}_h \rrbracket \llbracket \mathbf{v}_h \rrbracket \, d\gamma, \\ b_h(\mathbf{v}_h, p_h) &= - \int_{\Omega^{\#}} p_h \nabla \cdot \mathbf{v}_h \, d\mathbf{x} + \sum_{F \in \mathcal{F}_{int}^{\#} \cup \Gamma} \int_F \llbracket \mathbf{v}_h \rrbracket \cdot \mathbf{n}_F \{\{p_h\}\} \, d\gamma + \int_{\Gamma} \mathbf{v}_h \cdot \mathbf{n}_{\Gamma} p_h \, d\gamma, \end{aligned}$$

where  $\sigma > 0$  is the discontinuity-penalization function in  $L^{\infty}(\mathcal{F}_{int}^{\#} \cup \Gamma)$  that affects the stability of the method as well as the approximation quality and will be investigated below. This symmetric interior penalty parameter in the definition of  $a_h(\cdot, \cdot)$  will be sufficiently large in a sense that will be made precise later, see Lemma 4.2 and its proof below.

We note that the later formulation's disadvantage is that it is not well defined for  $H^1(\Omega^{\#})$  regularity, e.g. traces of functions defined in  $L^2(\Omega^{\#})$  are not well defined in  $\mathcal{F}_{int}^{\#}$ . The latter issue affects the terms  $\{\{\nabla(w)\}\}$ , and  $\nabla w \cdot \mathbf{n}_F$  in the sense that they are not well defined in  $H^1(\Omega^{\#})$ . This causes the need of additional regularity while the Galerkin orthogonality cannot be derived explicitly. In order to achieve optimal a priori error estimates, under the presence of terms such  $\{\{\nabla w\}\}_F$ ,  $\nabla w \cdot \mathbf{n}_F|_F$  which may involve  $\{\{\nabla(w - \pi_p w)\}\}_F$  and  $\nabla(w - \pi_p w) \cdot \mathbf{n}_F|_F$ , where  $\pi_p w$  is an operator  $\pi_p : H^{l_K}(\mathcal{K}) \rightarrow \mathcal{P}_p(\mathcal{K})$  an approximation of  $w$  for  $l_k \geq 0$  will be introduced in Lemma 4.3 and it is estimated optimally. We note at this point that the  $H^1(F)$  seminorm for an  $hp$ -a priori approximation error bound would require  $W^{1,\infty}$  norm error bounds which also requires further regularity, see for more details the work of [15]. To avoid the latter issue we employ proper bilinear form extensions. In particular we introduce the orthogonal  $L^2$ -projection in the FEM space  $S_{\mathcal{T}^{\#},.}^p$ , e.g.  $\Pi_{L^2} : (L^2(\Omega^{\#}))^d \rightarrow (S_{\mathcal{T}^{\#},.}^p)^d$  concluding in the

variational form:

$$\begin{aligned}\tilde{a}_h(\mathbf{u}_h, \mathbf{v}_h) &= \int_{\Omega^\sharp} \nabla \mathbf{u}_h : \nabla \mathbf{v}_h \, d\mathbf{x} - \sum_{F \in \mathcal{F}_{int}^\sharp \cup \Gamma} \int_F (\{\Pi_{\mathbf{L}^2}(\nabla \mathbf{u}_h)\} \cdot \mathbf{n}_F [\mathbf{v}_h] + \{\Pi_{\mathbf{L}^2}(\nabla \mathbf{v}_h)\} \cdot \mathbf{n}_F [\mathbf{u}_h]) \, d\gamma \\ &\quad - \int_{\Gamma} \mathbf{u}_h \Pi_{\mathbf{L}^2}(\nabla \mathbf{v}_h) \cdot \mathbf{n}_\Gamma \, d\gamma - \int_{\Gamma} \mathbf{v}_h \Pi_{\mathbf{L}^2}(\nabla \mathbf{u}_h) \cdot \mathbf{n}_\Gamma \, d\gamma + \int_{\Gamma} \sigma \mathbf{u}_h \mathbf{v}_h \, d\gamma + \sum_{F \in \mathcal{F}_{int}^\sharp \cup \Gamma} \int_F \sigma [\mathbf{u}_h] [\mathbf{v}_h] \, d\gamma, \\ b_h(\mathbf{v}_h, p_h) &= - \int_{\Omega^\sharp} p_h \nabla \cdot \mathbf{v}_h \, d\mathbf{x} + \sum_{F \in \mathcal{F}_{int}^\sharp \cup \Gamma} \int_F [\mathbf{v}_h] \cdot \mathbf{n}_F \{p_h\} \, d\gamma + \int_{\Gamma} \mathbf{v}_h \cdot \mathbf{n}_\Gamma p_h \, d\gamma\end{aligned}$$

respectively. For future reference, note that element-wise integration by parts in the previous forms yields the equivalent formulations

$$\begin{aligned}(2.4) \quad \tilde{a}_h(\mathbf{u}_h, \mathbf{v}_h) &= - \int_{\Omega^\sharp} \nabla \nabla \mathbf{u}_h \cdot \mathbf{v}_h \, d\mathbf{x} + \sum_{F \in \mathcal{F}_{int}^\sharp \cup \Gamma} \int_F [\Pi_{\mathbf{L}^2}(\nabla \mathbf{u}_h)] \cdot \mathbf{n}_F \{\mathbf{v}_h\} \, d\gamma \\ &\quad - \sum_{F \in \mathcal{F}_{int}^\sharp \cup \Gamma} \int_F \{\Pi_{\mathbf{L}^2}(\nabla \mathbf{v}_h)\} \cdot \mathbf{n}_F [\mathbf{u}_h] \, d\gamma - \int_{\Gamma} \mathbf{u}_h \Pi_{\mathbf{L}^2}(\nabla \mathbf{v}_h) \cdot \mathbf{n}_\Gamma \, d\gamma \\ &\quad + \int_{\Gamma} \sigma \mathbf{u}_h \mathbf{v}_h \, d\gamma + \sum_{F \in \mathcal{F}_{int}^\sharp \cup \Gamma} \int_F \sigma [\mathbf{u}_h] [\mathbf{v}_h] \, d\gamma,\end{aligned}$$

$$(2.5) \quad b_h(\mathbf{v}_h, p_h) = \int_{\Omega^\sharp} \mathbf{v}_h \cdot \nabla p_h \, d\mathbf{x} - \sum_{F \in \mathcal{F}_{int}^\sharp \cup \Gamma} \int_F \{\mathbf{v}_h\} \cdot \mathbf{n}_F [p_h] \, d\gamma,$$

which will be useful for asserting the consistency of the method.

Using the aforementioned weak formulation, an arbitrarily shape boundary elements discontinuous Galerkin method for (2.3) now reads as follows: Find  $(\mathbf{u}_h, p_h) \in V_h^\sharp \times Q_h^\sharp$ , such that

$$(2.6) \quad A_h(\mathbf{u}_h, p_h; \mathbf{v}_h, q_h) = L_h(\mathbf{v}_h, q_h), \quad \text{for all } (\mathbf{v}_h, q_h) \in V_h^\sharp \times Q_h^\sharp.$$

The bilinear and linear forms  $A_h$  and  $L_h$  are defined by

$$(2.7) \quad A_h(\mathbf{u}_h, p_h; \mathbf{v}_h, q_h) = \tilde{a}_h(\mathbf{u}_h, \mathbf{v}_h) + b_h(\mathbf{u}_h, q_h) + b_h(\mathbf{v}_h, p_h), \quad \text{and} \quad L_h(\mathbf{v}_h, q_h) = \int_{\Omega^\sharp} \mathbf{f} \cdot \mathbf{v}_h \, d\mathbf{x}.$$

We report that in the right hand side  $L_h(\mathbf{v}_h, q_h)$  we have omitted the zero Nitsche boundary terms, as well as,  $\tilde{a}_h(\mathbf{u}_h, \mathbf{v}_h) = a_h(\mathbf{u}_h, \mathbf{v}_h)$  when  $\mathbf{u}_h, \mathbf{v}_h \in V_h^\sharp$ .

### 3. PRELIMINARIES

Next, we define the discontinuity penalization parameter  $\sigma : \Gamma \cup \mathcal{F}_{int}^\sharp \rightarrow \mathbb{R}$ , the standard Sobolev norms and semi-norms on a domain  $\mathcal{X}$  for  $s \in \mathbb{N}$  will be denoted by  $\|\cdot\|_{s, \mathcal{X}}$  and  $|\cdot|_{s, \mathcal{X}}$ , respectively, omitting the index in case  $s = 0$ . The a-priori error bounds for the proposed unfitted dG method will be proved with respect to the following mesh-dependent norms:

$$\begin{aligned}\|\mathbf{v}\|^2 &= \|\nabla \mathbf{v}\|_{\Omega^\sharp}^2 + \|\sigma^{1/2} \mathbf{v}\|_{\Gamma}^2 + \sum_{F \in \Gamma} \|\mathbf{p}^{-1} h_F^{1/2} \nabla \mathbf{v} \cdot \mathbf{n}_F\|_F^2 \\ &\quad + \sum_{F \in \mathcal{F}_{int}^\sharp} \|\sigma^{1/2} [\mathbf{v}]\|_F^2 + \frac{1}{2} \sum_{K \in \mathcal{T}^{cov}} \|\mathbf{p}^{-1} h_K^{1/2} \nabla \mathbf{v} \cdot \mathbf{n}_T\|_{\partial K}^2, \\ \|p\|^2 &= \|p\|_{\Omega^\sharp}^2 + \sum_{F \in \Gamma} \|\mathbf{p}^{-1} h_F^{1/2} p\|_F^2 + \sum_{F \in \mathcal{F}_{int}^\sharp} \|\mathbf{p}^{-1} h_F^{1/2} [p]\|_F^2 + \frac{1}{2} \sum_{K \in \mathcal{T}^{cov}} \|\mathbf{p}^{-1} h_K^{1/2} p\|_{\partial K}^2,\end{aligned}$$

and  $\|(\mathbf{v}, p)\|^2 = \|\mathbf{v}\|^2 + \|p\|^2$ . To investigate stability, since some terms of the above terms dominate related to others, we will also make use of the following norms in  $\Omega^\sharp$  for the discrete velocity and pressure approximations, e.g. for the velocity norm the third and and fifth terms appear similar  $hp$ -behavior with the first term and for pressure the second, third and fourth term with the first term. For this reason, we also update and define the norms:

$$(3.1) \quad \|\mathbf{v}\|_{V^c}^2 = \|\nabla \mathbf{v}\|_{\Omega^{cov}}^2 + \|\sigma^{1/2} \mathbf{v}\|_{\Gamma}^2 + \sum_{F \in \mathcal{F}_{int}^\sharp} \|\sigma^{1/2} [\mathbf{v}]\|_F^2, \quad \text{and} \quad \|p\|_{Q^c}^2 = \|p\|_{\Omega^{cov}}^2,$$

while  $\|(\mathbf{v}, p)\|_{V^c, Q^c}^2 = \|\mathbf{v}\|_{V^c}^2 + \|p\|_{Q^c}^2$ . We underline, that in the following and for completeness we treat all the aforementioned terms showing this equivalence.

The following section is devoted to useful trace and inverse estimates, which have been proved in [15, 22] and they will form the basis to prove a-priori error estimates of the proposed method.

**3.1. Inverse estimates (trace and  $H^1-L^2$ ).** It is easy to derive the estimates with respect to the norms  $\|\cdot\|$  and  $\|\cdot\|_{V^c}$  or  $Q^c$ , namely,

$$(3.2) \quad \|\mathbf{v}\| \leq C_{V^c} \|\mathbf{v}\|_{V^c}, \quad \|p\| \leq C_{Q^c} \|p\|_{Q^c}.$$

**Assumption 3.1.** For each element  $K \in \mathcal{T}^\sharp$  with  $K \cap \Gamma \neq \emptyset$ , we assume that  $K$  is a Lipschitz domain, and  $\partial K$  can be subdivided into mutually exclusive subsets  $\{F_i\}_{i=1}^{n_K}$  characterized by the property that respective sub-elements  $K_{F_i} \equiv K_{F_i}(v_{0,i}) \subset K$  there exist, with  $d$  planar faces meeting at one vertex  $v_{0,i} \in K$ , with  $F_i \subset \partial K_{F_i}$ : for  $i = 1, \dots, n_K$ , we consider that (a)  $K_{F_i}$  is star-shaped with respect to  $v_{0,i}$ , and (b)  $\mathbf{d}_i(x) \cdot \mathbf{n}_{F_i}(x) > 0$  for  $\mathbf{d}_i(x) := x - v_{0,i}$ ,  $x \in K_{F_i}$ , and  $\mathbf{n}_{F_i}(x)$  the respective unit outward normal vector to  $F_i$  at  $x \in F_i$ . It is also considered that the boundary  $\partial K$  of each element  $K \in \mathcal{T}^\sharp$ ,  $K \cap \Gamma \neq \emptyset$  is the union of a finite number of closed  $C^1$  surfaces.

Both (a) and (b) assumptions, for the two dimensional case, are visualized in Figure 3. We notice that in the above weak mesh assumption, the sub-domains  $\{F_i\}_{i=1}^{n_K}$  are not required to coincide with the faces of the element  $K$ , namely, each  $F_i$  may be part of a face or may include one or more faces of  $K$ , as well as, there is no requirement for  $\{n_K\}_{K \in \mathcal{T}^\sharp, K \cap \Gamma \neq \emptyset}$  to remain uniformly bounded across the mesh. In particular Assumption 3.1 states that the curvature of the collection of consecutive curved faces comprising  $F_i$  cannot be arbitrarily large almost everywhere. Moreover, with some small loss of generality, Assumption 3.1 b) can be made stronger by adding the ingredient that it is possible to consider a fixed point  $v_{0,i}$  such that there exists a global constant  $c_{sh} > 0$ , such that

$$(3.3) \quad \mathbf{d}_i(x) \cdot \mathbf{n}_{F_i}(x) \geq c_{sh} h_{K_{F_i}}$$

see e.g. [24, 65]. We underline that (3.3) does not imply shape-regularity of the  $K_{F_i}$ 's; in particular  $K_{F_i}$ 's with small  $F_i$  compared to the remaining (straight) faces of  $K$  are acceptable. Such anisotropic boundary sub-elements  $K_{F_i}$ 's may be necessary to ensure that each  $K_{F_i}$  remains star-shaped when an element boundary's curvature is locally large, see e.g.,  $K_{F_i}$  in Figure 3 and a collection of both shape-regular and anisotropic  $K_{F_i}$ 's. In general,  $F_i$  is not required to be connected, although, by splitting  $F_i$  to its connected subsets, re-indexing the  $F_i$ 's to correspond to unique  $K_{F_i}$ , we can correspond one  $K_{F_i}$  to each  $F_i$ . The aforementioned Assumptions 3.1 are sufficient for the proof of the trace estimates as well as for the validity of the  $H^1-L^2$  inverse estimate as in [15].

**Lemma 3.2.** Let element  $K \in \mathcal{T}^\sharp$  be a Lipschitz domain satisfying Assumption 3.1. Then, for each  $F_i \subset \partial K$  from Assumptions 3.1,  $i = 1, \dots, n_K$ , and for each  $v \in \mathcal{P}^p(K)$ , we have the inverse estimate:

$$(3.4) \quad \|v\|_{F_i}^2 \leq \frac{(\mathfrak{p}+1)(\mathfrak{p}+d)}{\min_{x \in F_i} (\mathbf{d}_i \cdot \mathbf{n}_{F_i})} \|v\|_{K_{F_i}}^2.$$

**Remark 3.3.** Inequality (3.4) is a function of  $v_{0,i}$  defining  $K_{F_i}$ . The right-hand side can be minimized with a choice of an optimal  $v_{0,i}$ . We underline that under the stronger assumption (3.1), one could derive the trace inverse estimate for star-shaped, shape-regular elements with piecewise smooth boundaries:  $\|v\|_{\partial K}^2 \leq C \frac{\mathfrak{p}^2}{h_K} \|v\|_K^2$ .

**Lemma 3.4.** Let  $K \in \mathcal{T}^\sharp$  be a Lipschitz domain satisfying Assumption 3.1. Then, for all  $\varepsilon > 0$ , we have the estimate

$$\|v\|_{F_i}^2 \leq \frac{d + \varepsilon}{\min_{x \in F_i} (\mathbf{d}_i \cdot \mathbf{n}_{F_i})} \|v\|_{K_{F_i}}^2 + \frac{\max_{x \in F_i} |\mathbf{d}_i|_2^2}{\varepsilon \min_{x \in F_i} (\mathbf{d}_i \cdot \mathbf{n}_{F_i})} \|\nabla v\|_{K_{F_i}}^2,$$

for all  $v \in H^1(\Omega^\sharp)$  and  $i = 1, \dots, n_K$ . We note that summing over  $i = 1, \dots, n_K$ , under assumption  $\mathbf{d}_i(x) \cdot \mathbf{n}_{F_i}(x) \geq c_{sh} h_{K_{F_i}}$  and that  $h_{K_{F_i}} \sim h_K$  we take the estimate gives the classical trace estimate  $\|v\|_{\partial K}^2 \leq C(h_K^{-1} \|v\|_K^2 + h_K \|\nabla v\|_K^2)$ .

**Definition 3.5.** An element  $K \in \mathcal{T}^\sharp$  is said to be  $\mathfrak{p}$ -coverable with respect to  $\mathfrak{p} \in \mathbb{N}$ , if there exists a set of  $m_K$  overlapping shape regular simplices  $K_i$ ,  $i = 1, \dots, m_K$ ,  $m_K \in \mathbb{N}$ , such that

$$(3.5) \quad \text{dist}(K, \partial K_i) < C_{\text{as}} \frac{\text{diam}(K_i)}{\mathfrak{p}^2}, \text{ and } |K_i| \geq c_{\text{as}} |K|$$

for all  $i = 1, \dots, m_K$ , where  $C_{\text{as}}$  and  $c_{\text{as}}$  are positive constants, independent of  $K$  and  $\mathcal{T}^\sharp$ .

**Lemma 3.6** ([15]). *Let  $K \in \mathcal{T}^\sharp$  Lipschitz satisfying Assumption 3.1. Then, for each  $v \in \mathcal{P}^\mathfrak{p}(K)$ , we have the inverse inequality*

$$(3.6) \quad \|v\|_{F_i}^2 \leq C_{\text{INV}}(\mathfrak{p}, K, F_i) \frac{(\mathfrak{p}+1)(\mathfrak{p}+d)|F_i|}{|K|} \|v\|_K^2,$$

with  $C_{\text{INV}}(\mathfrak{p}, K, F_i)$  to be if  $K$  is  $\mathfrak{p}$ -coverable:  $\min\{\mathcal{C}(K, F_i), c_{\text{as}}^{-1} 2^{5d+1} \mathfrak{p}^{2(d-1)}\}$ , otherwise:  $\mathcal{C}(K, F_i)$ , with  $c_{\text{as}} > 0$  as in Definition 3.5 and  $\mathcal{C} = \frac{|K|}{|F_i|} \sup_{\mathbf{v}_{0,i} \in K} \min_{\mathbf{x} \in F_i} (\mathbf{d}_i \cdot \mathbf{n}_{F_i})$ .

We also recall from [15] the  $H^1-L^2$  inverse inequality for polynomials on a general curved element  $K \in \mathcal{T}^\sharp$ .

**Lemma 3.7.** *Let  $K \in \mathcal{T}^\sharp$  satisfy Assumptions 3.1. Then, for each  $v \in \mathcal{P}^\mathfrak{p}(K)$ , the inverse estimates hold, for  $K$   $\mathfrak{p}$ -coverable:*

$$(3.7) \quad \|\nabla v\|_K \leq C \frac{\mathfrak{p}^2}{h_K} \|v\|_K, \text{ and}$$

$$(3.8) \quad \|\nabla v \cdot \mathbf{n}_F\|_F \leq C' \frac{\mathfrak{p}^3}{h_K^{3/2}} \|v\|_K$$

hold, and the constants  $C, C'$  are dependent on the shape-regularity constant.

*Proof.* The first estimate comes immediately from [15] will the second comes from the algebraic calculations:  $\|\nabla v \cdot \mathbf{n}_F\|_F \leq C \frac{\mathfrak{p}}{h_K^{1/2}} \|\nabla v\|_K \leq C' \frac{\mathfrak{p}^2}{h_K} \frac{\mathfrak{p}}{h_K^{1/2}} \|v\|_K = C' \frac{\mathfrak{p}^3}{h_K^{3/2}} \|v\|_K$ .  $\square$

After defining the covering domain  $\bar{\Omega}^{\text{cov}}$  and considering the Assumption 3.9, see e.g. [15, 22], we interpolate a pair  $(\mathbf{u}, p) \in [H^2(\Omega^\sharp)]^d \times H^1(\Omega^\sharp)$  through a suitable interpolant of  $[H^{\mathfrak{p}+1}(\Omega^\sharp)]^d \times H^\mathfrak{p}(\Omega^\sharp)$ -extensions of the functions  $(\mathbf{u}, p)$  on  $\Omega^{\text{cov}}$ .

**Definition 3.8.** Given a mesh  $\mathcal{T}^\sharp$ , we define a covering  $\mathcal{T}^{\text{cov}} = \mathcal{K}$  of  $\mathcal{T}^\sharp$  to be a set of open shape-regular  $d$ -simplices  $\mathcal{K}$ , such that for each  $K \in \mathcal{T}^\sharp$ , there exists a  $\mathcal{K} \in \mathcal{T}^{\text{cov}}$  with  $K \subset \mathcal{K}$ . For a given  $\mathcal{T}^{\text{cov}}$ , we define the covering domain  $\bar{\Omega}^{\text{cov}} := \cup_{\mathcal{K} \in \mathcal{T}^{\text{cov}}} \bar{\mathcal{K}}$ .

**Assumption 3.9.** *For a given mesh  $\mathcal{T}^\sharp$ , we postulate the existence of a covering  $\mathcal{T}^{\text{cov}}$ , and of a global constant  $\mathcal{O}_{\Omega^\sharp} \in \mathbb{N}$ , independent of the mesh parameters, such that*

$$\max_{K \in \mathcal{T}} \text{card}\{K' \in \mathcal{T} : K' \cup K \neq \emptyset, K \in \mathcal{T}^{\text{cov}} \text{ such that } K \subset K'\} \leq \mathcal{O}_{\Omega^\sharp}.$$

For such  $\mathcal{T}^{\text{cov}}$ , we further assume that  $h_{\mathcal{K}} := \text{diam}(\mathcal{K}) \leq C_{\text{diam}} h_K$ , for all pairs  $K \in \mathcal{T}^\sharp, \mathcal{K} \in \mathcal{T}^{\text{cov}}$ , with  $K \subset \mathcal{K}$ , for a global constant  $C_{\text{diam}} > 0$ , uniformly with respect to the mesh size  $h_K$ .

The latter assumption provides the shape-regularity of the covering mesh  $\mathcal{T}^{\text{cov}}$  –not though for the true  $\mathcal{T}^\sharp$ – in the sense that there exists a positive constant  $c$ , independent of the mesh parameters, such that  $\forall K \in \mathcal{T}^{\text{cov}} \subset \mathcal{T}, \rho_{\mathcal{K}} \geq c h_{\mathcal{K}}$  holds, with  $\rho_{\mathcal{K}}$  denoting the diameter of the largest ball contained in  $\mathcal{K}$ . The aforementioned will allow the application of the standard  $hp$ -version approximation estimates on simplicial elements, see e.g., from [53] that on each  $\mathcal{K}$  we can restrict the error over  $K \subset \mathcal{K}$ . However, it requires to extend properly the exact solution  $u$  onto  $\Omega^{\text{cov}}$ . In particular:

**Theorem 3.10.** *Let  $\Omega^\sharp$  be a domain with a Lipschitz boundary. Then there exists a linear extension operator  $\mathfrak{E} : H^s(\Omega^\sharp) \rightarrow H^s(\mathbb{R}^d)$ ,  $s \in \mathbb{N}_0$ , such that  $\mathfrak{E}v|_{\Omega^\sharp} = v$  and*

$$\|\mathfrak{E}v\|_{H^s(\mathbb{R}^d)} \leq C_{\mathfrak{E}} \|v\|_{H^s(\Omega^\sharp)},$$

where  $C_{\mathfrak{E}}$  is a positive constant depending only on  $s$  and on  $\Omega^\sharp$ .

#### 4. STABILITY ESTIMATES

The fact that the discrete problem is well-posed follows by the inf-sup stability of the bilinear form  $A_h$  in the formulation (2.6) with respect to the  $\|\cdot\|_{V^c, Q^c}$  norm. We begin by investigating the properties of the separate forms which contribute to  $A_h$ . A useful observation is that the form  $\tilde{a}_h(\cdot, \cdot)$ , is continuous and coercive with respect to the norm  $\|\cdot\|_{V^c}$ . For this proof, we will use that the arbitrarily shaped boundary elements can be properly extended from the real domain  $\Omega^\sharp$  to the covering one,  $\Omega^{\text{cov}}$ .

**Lemma 4.1.** *There are constants  $C_u, C_p > 0$ , depending only on the shape-regularity and the polynomial order and not on the mesh or the location of the boundary, such that the following estimates hold:*

$$(4.1) \quad \|\nabla \mathbf{u}_h\|_{\mathcal{T}^{cov}}^2 \leq C_u \|\nabla \mathbf{v}_h\|_{\Omega^\sharp}^2 \leq C_u \|\nabla \mathbf{v}_h\|_{\mathcal{T}^{cov}}^2, \quad \text{for all } \mathbf{v}_h \in V_h^\sharp, \text{ and}$$

$$(4.2) \quad \|p_h\|_{\mathcal{T}^{cov}}^2 \leq C_p \|p_h\|_{\Omega^\sharp}^2 \leq C_p \|p_h\|_{\mathcal{T}^{cov}}^2, \quad \text{for all } p_h \in Q_h^\sharp.$$

*Proof.* Considering also the Assumption 3.1, we assume that there is an integer  $N > 0$  such that for each element  $K \in \mathcal{T}^{cov}$  with  $K \cap \Gamma \neq \emptyset$  there exists an element  $K' \in \mathcal{T}^{cov}$  with  $K' \cap \Gamma = \emptyset$  and at most  $N$  elements  $\{K\}_{i=1}^N$  such that  $K_1 = K$ ,  $K_N = K'$  and  $K_i \cap K_{i+1} \in \partial_i \mathcal{T}^{cov}$ ,  $i = 1, \dots, N-1$ . In particular, this means that the number of facets we need to cross so that we pass from the aforementioned element  $K$  to  $K' \subset \Omega^\sharp$  is bounded. Similar assumptions were made by [2], see also references therein, which ensure that  $\Gamma$  is reasonably resolved by  $\mathcal{T}^{cov}$ . For the first inequality (4.1) we compose the norm over  $\Omega^{cov}$  into sums over internal and boundary  $\mathcal{T}^{cov}$  elements,  $\|\cdot\|_{\mathcal{T}^{cov}} = \sum \|\cdot\|_{\mathcal{T}^{cov}\text{-boundary } K's} + \sum \|\cdot\|_{\mathcal{T}^{cov}\text{-internal } K's}$ . Let  $K_0$  be a boundary element of  $\mathcal{T}^{cov}$ . Then, there exists a  $K_N \subset \Omega^\sharp$  and at most  $N-1$   $\mathcal{T}^{cov}$ -boundary elements  $K_i$  and facets  $K_{i-1} \cap K_i = F_i$  that have to be overtaken in order to go across from  $K_0$  to  $K_N$ . Considering the aforementioned shape-regularity of the mesh, each facet corresponding to  $\mathcal{T}^{cov}$ -boundary elements  $F$  will only be involved in a finite number of such crossings. Additionally, let  $v$  be piecewise polynomial function defined on the extended element  $K = K_1 \cap K_2$ , and  $v_i$  to be the restriction of  $v$  to  $K_j$  for  $j = 1, 2$ . Then there is a constant  $C > 0$ , depending only on the shape-regularity of  $\mathcal{T}$  and the polynomial order  $\mathfrak{p} = \max(\mathfrak{p}_{v_1}, \mathfrak{p}_{v_2})$  of  $v$ , such that  $\|v\|_{K_1}^2 \leq C \|v\|_{K_2}^2$  as the two norms  $\|v_2\|_{K_1}$  and  $\|v_2\|_{K_2}$  are equivalent, by shape regularity. Here, each component of  $\nabla \mathbf{v}_h$  has been treated as  $v$  iteratively to each neighboring pair  $\{K_{i-1}, K_i\}$  and we take the desired estimate. The first inequality of (4.2) follows similarly following the same procedure for  $q_h$ . The second inequalities of (4.1)-(4.2) can be derived straight forward.  $\square$

With this preliminary result in place, we are now ready to prove discrete coercivity of  $\tilde{a}_h$  and continuity:

**Lemma 4.2.** *For suitably large discontinuity penalization parameter  $\sigma > 0$  in the definition of the bilinear form  $a_h(\cdot, \cdot)$ , there exists a constant  $c_a > 0$ , such that*

$$(4.3) \quad \tilde{a}_h(\mathbf{v}_h, \mathbf{v}_h) \geq c_{coer} \|\mathbf{v}_h\|_{V^\sharp}^2,$$

for any  $\mathbf{v}_h \in V_h^\sharp$ , and there exist constants  $C_a, C_b > 0$ , such that

$$(4.4) \quad \tilde{a}_h(\mathbf{u}_h, \mathbf{v}_h) \leq C_a \|\mathbf{u}_h\| \cdot \|\mathbf{v}_h\|, \quad \text{for every } \mathbf{u}_h, \mathbf{v}_h \in V_h^\sharp,$$

$$(4.5) \quad \tilde{a}_h(\mathbf{u}, \mathbf{v}_h) \leq C_a \|\mathbf{u}\| \cdot \|\mathbf{v}_h\|, \quad \text{for every } (\mathbf{u}, \mathbf{v}_h) \in ([H^{k+1}(\Omega^\sharp) \cap H_0^1(\Omega^\sharp)]^d + V_h^\sharp) \times V_h^\sharp,$$

$$(4.6) \quad b_h(\mathbf{u}, p_h) \leq C_b \|\mathbf{u}\| \cdot \|p_h\|, \quad \text{for every } (\mathbf{u}, p_h) \in ([H^{k+1}(\Omega^\sharp) \cap H_0^1(\Omega^\sharp)]^d + V_h^\sharp) \times Q_h^\sharp,$$

$$(4.7) \quad b_h(\mathbf{u}_h, p) \leq C_b \|\mathbf{u}_h\| \cdot \|p\|, \quad \text{for every } (\mathbf{u}_h, p) \in V_h^\sharp \times ([H^k(\Omega^\sharp) \cap L_0^2(\Omega^\sharp)] + Q_h^\sharp).$$

*Proof.* The proof is based on standard arguments. In particular, for any  $\lambda > 0$ , we have

$$\begin{aligned} \tilde{a}_h(\mathbf{v}_h, \mathbf{v}_h) &= \|\nabla \mathbf{v}_h\|_{\Omega^\sharp}^2 + \|\sigma^{1/2} \mathbf{v}_h\|_\Gamma^2 + \sum_{F \in \mathcal{F}_{int}^\sharp} \|\sigma^{1/2} [\mathbf{v}_h]\|_F^2 - 2 \int_\Gamma \mathbf{v}_h \mathbf{\Pi}_{\mathbf{L}^2}(\nabla \mathbf{v}_h) \cdot \mathbf{n}_\Gamma d\gamma \\ &\quad - 2 \sum_{F \in \mathcal{F}_{int}^\sharp} \int_F \{\mathbf{\Pi}_{\mathbf{L}^2}(\nabla \mathbf{v}_h)\} \cdot \mathbf{n}_F [\mathbf{v}_h] d\gamma \\ &\geq \|\nabla \mathbf{v}_h\|_{\Omega^\sharp}^2 + \|\sigma^{1/2} \mathbf{v}_h\|_\Gamma^2 + \sum_{F \in \mathcal{F}_{int}^\sharp} \|\sigma^{1/2} [\mathbf{v}_h]\|_F^2 - \lambda \sigma \|\sigma^{-1/2} \mathbf{\Pi}_{\mathbf{L}^2}(\nabla \mathbf{v}_h) \cdot \mathbf{n}_\Gamma\|_\Gamma^2 - \lambda^{-1} \sigma^{-1} \|\sigma^{1/2} \mathbf{v}_h\|_\Gamma^2 \\ &\quad - \lambda \sigma \sum_{F \in \mathcal{F}_{int}^\sharp} \|\sigma^{-1/2} \{\mathbf{\Pi}_{\mathbf{L}^2}(\nabla \mathbf{v}_h)\} \cdot \mathbf{n}_F\|_F^2 - \lambda^{-1} \sigma^{-1} \sum_{F \in \mathcal{F}_{int}^\sharp} \|\sigma^{1/2} [\mathbf{v}_h]\|_F^2 \\ &\geq \|\nabla \mathbf{v}_h\|_{\Omega^\sharp}^2 + (1 - \lambda^{-1} \sigma^{-1})(\|\sigma^{1/2} \mathbf{v}_h\|_\Gamma^2 + \sum_{F \in \mathcal{F}_{int}^\sharp} \|\sigma^{1/2} [\mathbf{v}_h]\|_F^2) \\ (4.8) \quad &\quad - \lambda \sigma \left( \sum_{F \in \mathcal{F}_{int}^\sharp} \|\sigma^{-1/2} \{\mathbf{\Pi}_{\mathbf{L}^2}(\nabla \mathbf{v}_h)\} \cdot \mathbf{n}_F\|_F^2 + \|\sigma^{-1/2} \mathbf{\Pi}_{\mathbf{L}^2}(\nabla \mathbf{v}_h) \cdot \mathbf{n}_\Gamma\|_\Gamma^2 \right). \end{aligned}$$

Young's inequality  $ab \leq a^2/(2\epsilon) + \epsilon b^2/2$  and inverse estimates (3.6), (3.8), are applied to the latter term in (4.8) to achieve a lower bound. In particular, note for  $F \in \mathcal{F}_{int}^\sharp$  with  $F = \partial K \cap \partial K'$  that

$$\begin{aligned} \|\sigma^{-1/2} \{\Pi_{\mathbf{L}^2}(\nabla \mathbf{v}_h)\} \cdot \mathbf{n}_F\|_F &\leq \frac{(\|\sigma^{-1/2} \Pi_{\mathbf{L}^2}(\nabla \mathbf{v}_h) \cdot \mathbf{n}_F\|_{F \subset \partial K} + \|\sigma^{-1/2} \Pi_{\mathbf{L}^2}(\nabla \mathbf{v}_h) \cdot \mathbf{n}_F\|_{F \subset \partial K'})}{2} \\ &\leq \frac{\mathfrak{p}^2 (C_{INV}(\mathfrak{p}, K, F_i) \frac{|F_i|}{|K|} \|\Pi_{\mathbf{L}^2}(\sigma^{-1/2} \nabla \mathbf{v}_h) \cdot \mathbf{n}_F\|_K^2 + C_{INV}(\mathfrak{p}, K', F_i) \frac{|F_i|}{|K'|} \|\Pi_{\mathbf{L}^2}(\sigma^{-1/2} \nabla \mathbf{v}_h) \cdot \mathbf{n}_F\|_{K'}^2)}{2} \\ &\leq \frac{1}{2} \mathfrak{p}^2 \max_{\kappa=K, K'} \{C_{INV}(\mathfrak{p}, \kappa, F_i) \frac{|F_i|}{|\kappa|} \|\sigma^{-1/2} \Pi_{\mathbf{L}^2}(\nabla \mathbf{v}_h)\|_\kappa\} \\ &\leq C_{\mathfrak{p}, 1} \max_{\kappa=K, K'} \{\|\sigma^{-1/2} \Pi_{\mathbf{L}^2}(\nabla \mathbf{v}_h)\|_\kappa\} \end{aligned}$$

and then summing over all faces in the active mesh,

$$(4.9) \quad \sum_{\substack{F \in \mathcal{F}_{int}^\sharp \\ F = \partial K \cap \partial K'}} \|\sigma^{-1/2} \{\Pi_{\mathbf{L}^2}(\nabla \mathbf{v}_h)\} \cdot \mathbf{n}_F\|_F^2 \leq C_{max} \|\nabla \mathbf{v}_h\|_{\Omega^\sharp}^2.$$

Likewise, using (3.8)

$$\begin{aligned} \|\sigma^{-1/2} \Pi_{\mathbf{L}^2}(\nabla \mathbf{v}_h) \cdot \mathbf{n}_\Gamma\|_\Gamma^2 &= \sum_{K \cap \Gamma \neq \emptyset} \|\sigma^{-1/2} \Pi_{\mathbf{L}^2}(\nabla \mathbf{v}_h) \cdot \mathbf{n}_\Gamma\|_{K \cap \Gamma}^2 \\ &\leq \sum_{K \cap \Gamma \neq \emptyset} \sigma^{-1/2} \sum_{i \in I_F^K} C_{INV}(\mathfrak{p}, K, F_i^K) \frac{\mathfrak{p}^2 |F_i|}{|K|} \|\Pi_{\mathbf{L}^2}(\nabla \mathbf{v}_h) \cdot \mathbf{n}_\Gamma\|_K^2 \\ &\leq \sum_{K \cap \Gamma \neq \emptyset} \sigma^{-1/2} |I_F^K| \max_{i \in I_F^K} \{C_{INV}(\mathfrak{p}, K, F_i^K)\} \frac{\mathfrak{p}^2 |F_i|}{|K|} \|\nabla \mathbf{v}_h\|_K^2 \\ (4.10) \quad &\leq C_{\mathfrak{p}, 2} \sum_{K \cap \Gamma \neq \emptyset} \|\nabla \mathbf{v}_h\|_K^2 \leq C'_{max} \|\nabla \mathbf{v}_h\|_{\Omega^\sharp}^2. \end{aligned}$$

Then, application of (4.1) verifies, for a suitable choice of  $\lambda$ , that the terms in (4.9) and (4.10) can be dominated by the leading two terms in (4.8). Indeed, letting  $C_{max}$  and  $C'_{max}$  the constants in (4.9) and (3.8) respectively and collecting all estimates, we conclude

$$\tilde{a}_h(\mathbf{v}_h, \mathbf{v}_h) \geq (C_u^{-1} - \lambda \sigma (C_{max} + C'_{max})) \|\nabla \mathbf{v}_h\|_{\Omega^\sharp}^2 + (1 - \lambda^{-1} \sigma^{-1}) (\|\sigma^{1/2} \mathbf{v}_h\|_\Gamma^2 + \sum_{F \in \mathcal{F}_{int}^\sharp} \|\sigma^{1/2} [\mathbf{v}_h]\|_F^2).$$

Coercivity (4.3) is already verified for  $1 > \lambda^{-1} \sigma^{-1} > C_u (C_{max} + C'_{max})$ , or  $1 < \lambda \sigma < C_u (C_{max} + C'_{max})$  which is valid for  $\lambda = (1 + C_u (C_{max} + C'_{max}) \mathfrak{p}^2)/(\sigma)$ . The corresponding coercivity constant is  $c_a = \min\{C_u^{-1} - \lambda \sigma (C_{max} + C'_{max}), 1 - \lambda^{-1} \sigma^{-1}\}$ .

The proof of the continuity is standard and it is omitted for brevity.  $\square$

We recall also from [15, 22] the following lemma and corollary that will be used next.

**Lemma 4.3.** *Let  $K \in \mathcal{T}^\sharp$  satisfy Assumptions 3.1 and 3.9, and let  $\mathcal{K} \in \mathcal{T}^{cov}$  be the corresponding simplex with  $K \subset \mathcal{K}$  as in Definition 3.8. Suppose that  $v \in L^2(\Omega^\sharp)$  is such that the extension  $\mathfrak{E}v|_{\mathcal{K}} \in H^{l_K}(\mathcal{K})$ , for some  $l_K \geq 0$ , and that Assumption 3.9 is satisfied. Then, there exists an operator  $\pi_{\mathfrak{p}} : H^{l_K}(\mathcal{K}) \rightarrow \mathcal{P}^\mathfrak{p}(\mathcal{K})$ , such that*

$$(4.11) \quad \|v - \pi_{\mathfrak{p}} v\|_{H^q(K)} \leq C_1 \frac{h_K^{s_K - q}}{\mathfrak{p}^{l_K - q}} \|\mathfrak{E}v\|_{H^{l_K}(\mathcal{K})},$$

for  $0 \leq q \leq l_K$ , and

$$(4.12) \quad \|v - \pi_{\mathfrak{p}} v\|_{F_i} \leq \mathcal{C}_{ap}^{\frac{1}{2}}(\mathfrak{p}, K, F_i) |F_i|^{\frac{1}{2}} \frac{h_K^{s_K - d/2}}{\mathfrak{p}^{l_K - 1/2}} \|\mathfrak{E}v\|_{H^{l_K}(\mathcal{K})}, \quad l_K \geq d/2,$$

with

$$\mathcal{C}_{ap}(\mathfrak{p}, K, F_i) := C_2 \min \left\{ \frac{h_K^d}{|F_i| \sup_{\mathbf{v}_{0,i} \in K} \min_{x \in F_i} (\mathbf{d}_i \cdot \mathbf{n})}, \mathfrak{p}^{d-1} \right\},$$

$s_K = \min\{\mathfrak{p} + 1, l_K\}$ , and  $C_1, C_2 > 0$  constants depending only on the shape-regularity of  $\mathcal{K}$ ,  $q$ ,  $l_K$ , on  $C_{diam}$  (from Assumption 3.9) and on the domain  $\Omega^\sharp$ .

We note the correspondence between  $\mathcal{C}_{\text{INV}}(\mathfrak{p}, K, F_i)$  from Lemma 3.6, and  $\mathcal{C}_{\text{ap}}(\mathfrak{p}, K, F_i)$  while  $h_K^d \sim |K|$  is the typical case. The key attribute of both expressions is that they remain bounded for degenerating  $|F_i|$ , allowing for the estimates (3.6) and (4.12) to remain finite as  $|F_i| \rightarrow 0$ .

**Corollary 4.4.** *The approximation errors of the extended interpolation operators  $\boldsymbol{\pi}_{\mathfrak{p}}$  and  $\pi_{\mathfrak{p}}$  for  $(\mathbf{u}, p) \in [H^{\mathfrak{p}+1}(\Omega^{\sharp})]^d \times H^{\mathfrak{p}}(\Omega^{\sharp})$  satisfy*

$$(4.13) \quad \|\mathbf{u} - \boldsymbol{\pi}_{\mathfrak{p}} \mathbf{u}\| \leq C \sum_{K \in \mathcal{T}^{\sharp}} \frac{h_K^{\mathfrak{p}}}{\mathfrak{p}^{\mathfrak{p}-\frac{1}{2}}} \|\mathbf{u}\|_{\mathfrak{p}+1, K},$$

$$(4.14) \quad \|(\mathbf{u} - \boldsymbol{\pi}_{\mathfrak{p}} \mathbf{u}, p - \pi_{\mathfrak{p}} p)\| \leq C \sum_{K \in \mathcal{T}^{\sharp}} \frac{h_K^{\mathfrak{p}}}{\mathfrak{p}^{\mathfrak{p}-\frac{1}{2}}} \left( \|\mathbf{u}\|_{\mathfrak{p}+1, K} + \frac{1}{\mathfrak{p}^{\frac{1}{2}}} \|p\|_{\mathfrak{p}, K} \right).$$

*Proof.* It is convenient to introduce the auxiliary norm

$$\begin{aligned} \|\mathbf{v}\|_h^2 &= \sum_{\mathcal{K} \in \mathcal{T}^{\text{cov}}} \|\nabla v\|_{\mathcal{K}}^2 + \|\sigma^{1/2} \mathbf{v}\|_{\Gamma}^2 + \sum_{F \in \mathcal{T}^{\sharp} \cap \Gamma} \|\mathfrak{p}^{-1} h_F^{1/2} \mathbf{n}_F \cdot \nabla \mathbf{v}\|_F^2 + \sum_{F \in \mathcal{F}_{\text{int}}^{\sharp}} \|\sigma^{1/2} [\mathbf{v}]\|_F^2 \\ &\quad + \frac{1}{2} \sum_{K \in \mathcal{T}^{\text{cov}}} \|\mathfrak{p}^{-1} h_K^{1/2} \nabla \mathbf{v}|_K \cdot \mathbf{n}_{\partial K}\|_{\partial K}^2, \end{aligned}$$

see also [15, p.60]. This norm clearly bounds  $\|\mathbf{v}\|$ , in the sense that  $\|\mathbf{v} - \boldsymbol{\pi}_{\mathfrak{p}} \mathbf{v}\| \leq \|\mathfrak{E}^{\mathfrak{p}+1} \mathbf{v} - \boldsymbol{\pi}_{\mathfrak{p}} \mathbf{v}\|_h$ . Hence, we may prove the estimate for  $\|\cdot\|_h$  instead of  $\|\cdot\|$ . Setting  $\mathbf{e}_{\pi} = \mathfrak{E}^{\mathfrak{p}+1} \mathbf{u} - \boldsymbol{\pi}_{\mathfrak{p}} \mathbf{u}$ , we take by definition

$$\begin{aligned} \|\mathbf{e}_{\pi}\|_h^2 &= \sum_{\mathcal{K} \in \mathcal{T}^{\text{cov}}} \|\nabla \mathbf{e}_{\pi}\|_{\mathcal{K}}^2 + \|\sigma^{1/2} \mathbf{e}_{\pi}\|_{\Gamma}^2 + \sum_{F \in \mathcal{T}^{\sharp} \cap \Gamma} \|\mathfrak{p}^{-1} h_F^{1/2} \nabla \mathbf{e}_{\pi} \cdot \mathbf{n}_F\|_F^2 + \sum_{F \in \mathcal{F}_{\text{int}}^{\sharp}} \|\sigma^{1/2} [\mathbf{e}_{\pi}]\|_F^2 \\ &\quad + \sum_{F \in \mathcal{F}_{\text{int}}^{\sharp}} \|\mathfrak{p}^{-1} h_F^{1/2} \{\nabla \mathbf{e}_{\pi}\} \cdot \mathbf{n}_F\|_F^2. \end{aligned}$$

All the above terms may be estimated, using the local approximation properties (4.11)–(4.12), the aforementioned inverse estimates and the stability of the extension operator  $\mathfrak{E}^{k+1}$ . For instance,

$$\sum_{\mathcal{K} \in \mathcal{T}^{\text{cov}}} \|\nabla \mathbf{e}_{\pi}\|_{\mathcal{K}} \leq \sum_{\mathcal{K} \in \mathcal{T}^{\text{cov}}} \|\mathbf{e}_{\pi}\|_{H^1(\mathcal{K})} \stackrel{(4.11)}{\leq} C \sum_{\mathcal{K} \in \mathcal{T}^{\text{cov}}} \frac{h_{\mathcal{K}}^{\mathfrak{p}}}{\mathfrak{p}^{\mathfrak{p}}} \|\mathfrak{E} u\|_{H^{\mathfrak{p}+1}(\mathcal{K})},$$

after choosing  $q = 1$ ,  $l_k = \mathfrak{p} + 1$  and  $s^k = \min(\mathfrak{p} + 1, l_k)$  in (4.11). Similarly, we derive

$$\sum_{F \in \mathcal{T}^{\sharp} \cap \Gamma} \|\mathfrak{p} h_F^{-1/2} \mathbf{e}_{\pi}\|_F \stackrel{(4.12)}{\leq} C \sum_{\mathcal{K} \in \mathcal{T}^{\text{cov}}} \mathfrak{p} h_{\mathcal{K}}^{-1/2} \frac{h_{\mathcal{K}}^{\mathfrak{p}+1/2}}{\mathfrak{p}^{\mathfrak{p}+1/2}} \|\mathfrak{E} u\|_{H^{\mathfrak{p}+1}(\mathcal{K})} = C \sum_{\mathcal{K} \in \mathcal{T}^{\text{cov}}} \frac{h_{\mathcal{K}}^{\mathfrak{p}}}{\mathfrak{p}^{\mathfrak{p}-\frac{1}{2}}} \|\mathfrak{E} u\|_{H^{\mathfrak{p}+1}(\mathcal{K})},$$

e.g. for  $d = 2$ ,  $l_k = \mathfrak{p} + 1$ . Let  $F \subset \partial K$ . As we have seen in the variational formulation, the norm  $\|\nabla e_p \cdot \mathbf{n}_F\|_F$  can be efficiently approximated by  $\|\nabla e_p \cdot \mathbf{n}_F\|_F \leq C \frac{\mathfrak{p}}{h_K^{1/2}} \|\nabla e_p\|_{L^2(K)}$ . We note that inserting the  $\Pi_{L^2}$  projection we are loosing  $\mathfrak{p}^{1/2}$  accuracy, [29], although this is consistent with the half power we loose from the penalization of the method and we can prove optimal a priori error bounds. Finally we take

$$\sum_{F \in \mathcal{T}^{\sharp} \cap \Gamma} \|\mathfrak{p}^{-1} h_F^{1/2} \cdot \nabla e_p \cdot \mathbf{n}_F\|_F \leq C \sum_{\mathcal{K} \in \mathcal{T}^{\text{cov}}} \mathfrak{p}^{-1} h_{\mathcal{K}}^{1/2} \frac{\mathfrak{p}}{h_{\mathcal{K}}^{1/2}} \|\nabla e_p\|_{\mathcal{K}} \leq C \sum_{\mathcal{K} \in \mathcal{T}^{\text{cov}}} \frac{h_{\mathcal{K}}^{\mathfrak{p}}}{\mathfrak{p}^{\mathfrak{p}}} \|\mathfrak{E} u\|_{H^{\mathfrak{p}+1}(\mathcal{K})}.$$

Proceeding in a similar fashion, we have

$$\begin{aligned} \sum_{F \in \mathcal{F}_{\text{int}}^{\sharp}} \|\sigma [\mathbf{e}_{\pi}]\|_F &= \sum_{F \in \mathcal{F}_{\text{int}}^{\sharp}} \|\mathfrak{p} h_F^{-1/2} [\mathbf{e}_{\pi}]\|_F \leq C \sum_{\mathcal{K} \in \mathcal{T}^{\text{cov}}} \frac{h_{\mathcal{K}}^{\mathfrak{p}}}{\mathfrak{p}^{\mathfrak{p}-\frac{1}{2}}} \|\mathfrak{E} u\|_{H^{\mathfrak{p}+1}(\mathcal{K})}, \\ \sum_{F \in \mathcal{F}_{\text{int}}^{\sharp}} \|\mathfrak{p}^{-1} h_F^{1/2} \{\nabla \mathbf{e}_{\pi}\} \cdot \mathbf{n}_F\|_F^2 &\leq C \sum_{\mathcal{K} \in \mathcal{T}^{\text{cov}}} \frac{h_{\mathcal{K}}^{\mathfrak{p}}}{\mathfrak{p}^{\mathfrak{p}}} \|\mathfrak{E} u\|_{H^{\mathfrak{p}+1}(\mathcal{K})}, \end{aligned}$$

and the proof of (4.14) is complete. The proof of the estimate (4.14) for the approximation error in the product space is similar, considering the auxiliary pressure norm

$$\|p\|_h^2 = \sum_{\mathcal{K} \in \mathcal{T}^{\text{cov}}} \|p\|_{\mathcal{K}}^2 + \sum_{F \in \mathcal{T}^{\sharp} \cap \Gamma} \|\mathfrak{p}^{-1} h_F^{1/2} p\|_F^2 + \sum_{F \in \mathcal{F}_{\text{int}}^{\sharp}} \|\mathfrak{p}^{-1} h_F^{1/2} [p]\|_F^2$$

and proving the assertion for  $e_\pi = \|\mathfrak{E}p - \pi_{\mathfrak{p}} p\|_h$ . In particular we can employ a multiplicative trace inequality:

$$\|q\|_{\partial K}^2 \leq C(\|q\|_K \|\nabla q\|_K + h_K^{-1} \|q\|_K^2), \quad q \in H^1(K),$$

[32, p2140], [56, p1571], and we conclude to

$$\begin{aligned} \sum_{F \in \mathcal{T}^\sharp} \|\mathfrak{p}^{-1} h_F^{1/2} e_\pi\|_F^2 &\leq C \sum_{K \in \mathcal{T}^\sharp} (\|\mathfrak{p}^{-1} h_K^{1/2} e_\pi\|_K \|\mathfrak{p}^{-1} h_K^{1/2} \nabla e_\pi\|_K + h_K^{-1} \|\mathfrak{p}^{-1} h_K^{1/2} e_\pi\|_K^2) \\ &\stackrel{q=0, s_K=l_K=\mathfrak{p}}{\leq} C \sum_{\substack{K \in \mathcal{T}^{cov} \\ K \in \mathcal{T}^\sharp}} \left( \frac{h_K^{s_K-0}}{\mathfrak{p}^{\mathfrak{p}-0}} \|\mathfrak{p}^{-1} h_K^{1/2} \mathfrak{E}p\|_{H^{\mathfrak{p}}(K)} \|\mathfrak{p}^{-1} h_K^{1/2} \nabla e_\pi\|_K + h_K^{-1} \|\mathfrak{p}^{-1} h_K^{1/2} e_\pi\|_K^2 \right) \\ &\leq C \sum_{\substack{K \in \mathcal{T}^{cov} \\ K \in \mathcal{T}^\sharp}} \left( \frac{h_K^{\mathfrak{p}}}{\mathfrak{p}^{\mathfrak{p}}} \|\mathfrak{p}^{-1} h_K^{1/2} \mathfrak{E}p\|_{H^{\mathfrak{p}}(K)} \frac{\mathfrak{p}^2}{h_K} \|\mathfrak{p}^{-1} h_K^{1/2} e_\pi\|_K + h_K^{-1} \|\mathfrak{p}^{-1} h_K^{1/2} e_\pi\|_K^2 \right) \\ &\leq C \sum_{\substack{K \in \mathcal{T}^{cov} \\ K \in \mathcal{T}^\sharp}} \left( \frac{h_K^{\mathfrak{p}}}{\mathfrak{p}^{\mathfrak{p}}} \|\mathfrak{p}^{-1} h_K^{1/2} \mathfrak{E}p\|_{H^{\mathfrak{p}}(K)} \frac{\mathfrak{p}}{h_K^{1/2}} \|e_\pi\|_K + \mathfrak{p}^{-2} \|e_\pi\|_K^2 \right), \end{aligned}$$

and finally with standard algebra

$$\begin{aligned} \sum_{F \in \mathcal{T}^\sharp} \|\mathfrak{p}^{-1} h_F^{1/2} e_\pi\|_F^2 &\leq C \sum_{\substack{K \in \mathcal{T}^{cov} \\ K \in \mathcal{T}^\sharp}} \left( \frac{h_K^{\mathfrak{p}}}{\mathfrak{p}^{\mathfrak{p}}} \|\mathfrak{E}p\|_{H^{\mathfrak{p}}(K)} \|e_\pi\|_K + \mathfrak{p}^{-2} \|e_\pi\|_K^2 \right) \\ &\leq C \sum_{K \in \mathcal{T}^{cov}} \left( \frac{h_K^{\mathfrak{p}}}{\mathfrak{p}^{\mathfrak{p}}} \|\mathfrak{E}p\|_{H^{\mathfrak{p}}(K)} \frac{h_K^{\mathfrak{p}}}{\mathfrak{p}^{\mathfrak{p}}} \|\mathfrak{E}p\|_{H^{\mathfrak{p}}(K)} + \mathfrak{p}^{-2} \frac{h_K^{2\mathfrak{p}}}{\mathfrak{p}^{2\mathfrak{p}}} \|\mathfrak{E}p\|_{H^{\mathfrak{p}}(K)}^2 \right) \\ &\leq C \sum_{K \in \mathcal{T}^{cov}} \left( \frac{h_K^{2\mathfrak{p}}}{\mathfrak{p}^{2\mathfrak{p}}} \|\mathfrak{E}p\|_{H^{\mathfrak{p}}(K)}^2 + \frac{h_K^{2\mathfrak{p}}}{\mathfrak{p}^{2(\mathfrak{p}+1)}} \|\mathfrak{E}p\|_{H^{\mathfrak{p}}(K)}^2 \right) \\ &\leq C \sum_{K \in \mathcal{T}^{cov}} \frac{h_K^{2\mathfrak{p}}}{\mathfrak{p}^{2\mathfrak{p}}} \|\mathfrak{E}p\|_{H^{\mathfrak{p}}(K)}^2, \end{aligned}$$

which completes the proof.  $\square$

We continue with the stability for the  $b_h$  proof.

**Lemma 4.5.** *There exists  $C > 0$ , such that for every  $p_h \in Q_h^\sharp$  we have*

$$(4.15) \quad C \|p_h\|_{\Omega^\sharp} \leq \sup_{\mathbf{w}_h \in V_h^\sharp \setminus \{0\}} \frac{b_h(\mathbf{w}_h, p_h)}{\|\mathbf{w}_h\|_{V^c}} + \left( \sum_{K \in \mathcal{T}^\sharp} \|\mathfrak{p}^{-2} h_K \nabla p_h\|_K^2 \right)^{1/2} + \left( \sum_{F \in \mathcal{F}_{int}^\sharp} \left\| \mathfrak{p}^{-1} h_F^{1/2} \llbracket p_h \rrbracket \right\|_F^2 \right)^{1/2}.$$

*Proof.* Considering a fixed  $p_h \in Q_h^\sharp$ , due to the surjectivity of the divergence operator there exists a  $\mathbf{v}_{p_h} \in [H_0^1(\Omega^\sharp)]^d$ , such that

$$(4.16) \quad \nabla \cdot \mathbf{v}_{p_h} = p_h \quad (\text{a}) \quad \text{and} \quad C_{\Omega^\sharp} \|\mathbf{v}_{p_h}\|_{1, \Omega^\sharp} \leq \|p_h\|_{\Omega^\sharp} \quad (\text{b})$$

for some constant  $C_{\Omega^\sharp} > 0$ . Then, applying integration by parts on each element and the fact that  $\mathbf{v}_{p_h}$  and  $\llbracket \mathbf{v}_{p_h} \rrbracket$  vanish on  $\Gamma$  and on  $F \in \mathcal{F}_{int}^\sharp$  respectively –since  $\mathbf{v}_{p_h} \in [H_0^1(\Omega^\sharp)]^d$  is an element of the continuous space– implies

$$\begin{aligned} \|p_h\|_{\Omega^\sharp}^2 &= \int_{\Omega^\sharp} p_h (\nabla \cdot \mathbf{v}_{p_h}) \, d\mathbf{x} = - \int_{\Omega^\sharp} \mathbf{v}_{p_h} \nabla p_h \, d\mathbf{x} + \sum_{K \in \mathcal{T}^\sharp} \int_{\partial K} (\mathbf{v}_{p_h} \cdot \mathbf{n}_F) p_h \, d\mathbf{x} \\ &= - \int_{\Omega^\sharp} \mathbf{v}_{p_h} \nabla p_h \, d\mathbf{x} + \sum_{F \in \mathcal{F}_{int}^\sharp} \int_F \{\mathbf{v}_{p_h}\} \cdot \mathbf{n}_F \llbracket p_h \rrbracket \, d\gamma + \sum_{F \in \mathcal{F}_{int}^\sharp} \int_F \llbracket \mathbf{v}_{p_h} \rrbracket \cdot \mathbf{n}_F \{\mathbf{v}_{p_h}\} \, d\gamma \\ &\quad + \int_{\Gamma \cap K} (\mathbf{v}_{p_h} \cdot \mathbf{n}_\Gamma) p_h \, d\gamma \\ &= - \int_{\Omega^\sharp} \mathbf{v}_{p_h} \nabla p_h \, d\mathbf{x} + \sum_{F \in \mathcal{F}_{int}^\sharp} \int_F \{\mathbf{v}_{p_h}\} \cdot \mathbf{n}_F \llbracket p_h \rrbracket \, d\gamma. \end{aligned}$$

Next, we introduce the interpolation error  $\mathbf{e}_h := \Pi_h \mathbf{v}_{p_h} - \mathbf{v}_{p_h}$  for  $\mathbf{v}_{p_h} \mapsto \Pi_h \mathbf{v}_{p_h} \in V_h^\sharp$  in the previous expression and holds that

$$(4.17) \quad \begin{aligned} \|p_h\|_{\Omega^\sharp}^2 &= \int_{\Omega^\sharp} \mathbf{e}_h \nabla p_h \, d\mathbf{x} - \int_{\Omega^\sharp} \Pi_h \mathbf{v}_{p_h} \nabla p_h \, d\mathbf{x} + \sum_{F \in \mathcal{F}_{int}^\sharp} \int_F \{\!\{ \mathbf{v}_{p_h} \}\!\} \cdot \mathbf{n}_F \llbracket p_h \rrbracket \, d\gamma \\ &\stackrel{(2.5)}{=} \int_{\Omega^\sharp} \mathbf{e}_h \nabla p_h \, d\mathbf{x} - b_h(\Pi_h \mathbf{v}_{p_h}, p_h) - \sum_{F \in \mathcal{F}_{int}^\sharp} \int_F \{\!\{ \mathbf{e}_h \}\!\} \cdot \mathbf{n}_F \llbracket p_h \rrbracket \, d\gamma. \end{aligned}$$

For the first term, the Cauchy–Schwarz inequality, (4.11) and (4.16)a, yields

$$(4.18) \quad \begin{aligned} \left| \int_{\Omega^\sharp} \mathbf{e}_h \nabla p_h \, d\mathbf{x} \right| &\leq \left( \sum_{K \in \mathcal{T}^\sharp} \|\mathfrak{p} h_K^{-1/2} \mathbf{e}_h\|_K^2 \right)^{1/2} \left( \sum_{K \in \mathcal{T}^\sharp} \|\mathfrak{p}^{-1} h_K^{1/2} \nabla p_h\|_K^2 \right)^{1/2} \\ &\stackrel{(4.11)}{\leq} C \|\mathbf{v}_{p_h}\|_{1, \Omega^\sharp} \left( \sum_{K \in \mathcal{T}^\sharp} \|\mathfrak{p}^{-1} h_K^{1/2} \nabla p_h\|_K^2 \right)^{1/2} \stackrel{(4.16)a}{\leq} C C_{\Omega^\sharp}^{-1} \|p_h\|_{\Omega^\sharp} \left( \sum_{K \in \mathcal{T}^\sharp} \|\mathfrak{p}^{-1} h_K^{1/2} \nabla p_h\|_K^2 \right)^{1/2}. \end{aligned}$$

Employing the continuity property of the extended interpolation operator and (4.16),

$$(4.19) \quad \begin{aligned} |b_h(\Pi_h \mathbf{v}_{p_h}, p_h)| &= \frac{|b_h(\Pi_h \mathbf{v}_{p_h}, p_h)|}{\|\Pi_h \mathbf{v}_{p_h}\|_{V^c}} \|\Pi_h \mathbf{v}_{p_h}\|_{V^c} \leq \left( \sup_{\mathbf{w}_h \in V_h^\sharp \setminus \{0\}} \frac{b_h(\mathbf{w}_h, p_h)}{\|\mathbf{w}_h\|_{V^c}} \right) C_{proj} \|\mathbf{v}_{p_h}\|_{1, \Omega^\sharp} \\ &\leq \left( \sup_{\mathbf{w}_h \in V_h^\sharp \setminus \{0\}} \frac{b_h(\mathbf{w}_h, p_h)}{\|\mathbf{w}_h\|_{V^c}} \right) C_{proj} C_{\Omega^\sharp}^{-1} \|p_h\|_{\Omega^\sharp}. \end{aligned}$$

To handle the third term, we follow the steps similarly as we did for the first term using (4.12) and we conclude to

$$(4.20) \quad \begin{aligned} \left| \sum_{F \in \mathcal{F}_{int}^\sharp} \int_F \{\!\{ \mathbf{e}_h \}\!\} \cdot \mathbf{n}_F \llbracket p_h \rrbracket \, d\gamma \right| &\leq \left( \sum_{F \in \mathcal{F}_{int}^\sharp} \|\mathfrak{p} h_F^{-1/2} \{\!\{ \mathbf{e}_h \}\!\}\|_F^2 \right)^{1/2} \left( \sum_{F \in \mathcal{F}_{int}^\sharp} \|\mathfrak{p}^{-1} h_F^{1/2} \llbracket p_h \rrbracket\|_F^2 \right)^{1/2} \\ &\leq C \|\mathbf{v}_{p_h}\|_{1, \Omega^\sharp} \left( \sum_{F \in \mathcal{F}_{int}^\sharp} \|\mathfrak{p}^{-1} h_F^{1/2} \llbracket p_h \rrbracket\|_F^2 \right)^{1/2} \leq C C_{\Omega^\sharp}^{-1} \|p_h\|_{\Omega^\sharp} \left( \sum_{F \in \mathcal{F}_{int}^\sharp} \|\mathfrak{p}^{-1} h_F^{1/2} \llbracket p_h \rrbracket\|_F^2 \right)^{1/2}. \end{aligned}$$

Finally, we collect the inequalities (4.18)–(4.20), and the proof is completed.  $\square$

An instant conclusion is the following.

**Corollary 4.6.** *For every  $p_h \in Q_h^\sharp$ , there exists  $\mathbf{w}_h \in V_h^\sharp$ , such that*

$$(4.21) \quad b_h(\mathbf{w}_h, -p_h) \geq \|p_h\|_{\Omega^\sharp}^2 - C_\sigma \left( \left( \sum_{K \in \mathcal{T}^\sharp} \|\mathfrak{p}^{-2} h_K \nabla p_h\|_K^2 \right)^{1/2} + \left( \sum_{F \in \mathcal{F}_{int}^\sharp} \|\mathfrak{p}^{-1} h_F^{1/2} \llbracket p_h \rrbracket\|_F^2 \right)^{1/2} \right) \|p_h\|_{\Omega^\sharp},$$

for suitable  $C_\sigma > 0$ .

*Proof.* We denote by  $C_1, C_2$  the constants appearing in (4.18), (4.20), we rearrange (4.17) and we derive  $b_h(\Pi_h \mathbf{v}_{p_h}, -p_h) \geq \|p_h\|_{\Omega^\sharp}^2 - \left| \int_{\Omega^\sharp} \mathbf{e}_h \nabla p_h \, d\mathbf{x} \right| - \left| \sum_{F \in \mathcal{F}_{int}^\sharp} \int_F \{\!\{ \mathbf{e}_h \}\!\} \cdot \mathbf{n}_F \llbracket p_h \rrbracket \, d\gamma \right|$ , hence, the result clearly follows for  $\mathbf{w}_h = \Pi_h \mathbf{v}_{p_h}$  with  $C_\sigma = \max\{C_1, C_2\}$ .  $\square$

Next, we pass to the discrete inf–sup stability which is being proven below.

**Theorem 4.7.** *There is a constant  $c_{bil} > 0$ , such that for all  $(\mathbf{u}_h, p_h) \in V_h^\sharp \times Q_h^\sharp$ , we have*

$$(4.22) \quad c_{bil} \|\llbracket (\mathbf{u}_h, p_h) \rrbracket\|_{V^c, Q^c} \leq \sup_{(\mathbf{v}_h, q_h) \in V_h^\sharp \times Q_h^\sharp} \frac{A_h(\mathbf{u}_h, p_h; \mathbf{v}_h, q_h)}{\|\llbracket (\mathbf{v}_h, q_h) \rrbracket\|_{V^c, Q^c}}.$$

*Proof.* Similar to [2], let  $(\mathbf{u}_h, p_h) \in V_h^\sharp \times Q_h^\sharp$  and note by Corollary 4.6 that there exists  $\mathbf{w}_h \in V_h^\sharp$  in (4.21). A matter of fact, there is no loss of generality in setting  $\|\mathbf{w}_h\|_{V^c} = \|p_h\|_{\Omega^\sharp}$  and then inequality

(4.21) combined with the Young inequality and factorizing with respect to  $\|p_h\|_{\Omega^\sharp}^2$  we obtain

$$\begin{aligned}
 b_h(\mathbf{w}_h, -p_h) &\geq \left(1 - \frac{C_\sigma \lambda}{2}\right) \|p_h\|_{\Omega^\sharp}^2 - \frac{C_\sigma}{2\lambda} \left( \left( \sum_{K \in \mathcal{T}^\sharp} \|\mathfrak{p}^{-2} h_K \nabla p_h\|_K^2 \right)^{1/2} + \left( \sum_{F \in \mathcal{F}_{int}^\sharp} \|\mathfrak{p}^{-1} h_F^{1/2} \llbracket p_h \rrbracket\|_F^2 \right)^{1/2} \right)^2 \\
 (4.23) \quad &\geq \left(1 - \frac{C_\sigma \lambda}{2}\right) \|p_h\|_{\Omega^\sharp}^2 - \frac{C_\sigma}{\lambda} \sum_{K \in \mathcal{T}^\sharp} \|\mathfrak{p}^{-2} h_K \nabla p_h\|_K^2 - \frac{C_\sigma}{\lambda} \sum_{F \in \mathcal{F}_{int}^\sharp} \|\mathfrak{p}^{-1} h_F^{1/2} \llbracket p_h \rrbracket\|_F^2.
 \end{aligned}$$

We focus now on showing that for a sensible choice of parameters  $\zeta_1 > 0$  and  $\zeta_2 > 0$ , there exists a constant  $c_{bil} > 0$  such that the test pair  $(\mathbf{v}_h, q_h) = (\mathbf{u}_h, -p_h) + \zeta_1(-\mathbf{w}_h, 0) + \zeta_2(-\mathfrak{p}^{-4}\theta \nabla p_h, 0)$ , for proper  $\theta \in \mathbb{R}$  that will be chosen later, yields

$$(4.24) \quad A_h(\mathbf{u}_h, p_h; \mathbf{v}_h, q_h) \geq c_{bil} \|\mathbf{u}_h\|_{V^c} \|\mathbf{v}_h\|_{V^c},$$

whereby the desired outcome (4.22) is then provided.

Consequently, if we initially test with  $(\mathbf{u}_h, -p_h)$  using the coercivity estimate (4.3) of  $\tilde{a}_h$ , we derive

$$(4.25) \quad A_h(\mathbf{u}_h, p_h; \mathbf{u}_h, -p_h) = \tilde{a}_h(\mathbf{u}_h, \mathbf{u}_h) \geq c_a \|\mathbf{u}_h\|_{V^c}^2.$$

Thus, we consider  $(-\mathbf{w}_h, 0)$  in (4.23) and utilize the continuity estimate (4.4) of  $\tilde{a}_h$  together with the Young inequality,

$$\begin{aligned}
 A_h(\mathbf{u}_h, p_h; -\mathbf{w}_h, 0) &= -\tilde{a}_h(\mathbf{u}_h, \mathbf{w}_h) + b_h(\mathbf{w}_h, -p_h) \geq -\frac{C_a}{2\lambda} \|\mathbf{u}_h\|_{V^c}^2 + \left(1 - \frac{C_a \lambda}{2} - \frac{C_\sigma \lambda}{2}\right) \|p_h\|_{\Omega^\sharp}^2 \\
 &\quad - \frac{C_\sigma}{\lambda} \sum_{K \in \mathcal{T}^\sharp} \|\mathfrak{p}^{-2} h_K \nabla p_h\|_K^2 - \frac{C_\sigma}{\lambda} \sum_{F \in \mathcal{F}_{int}^\sharp} \|\mathfrak{p}^{-1} h_F^{1/2} \llbracket p_h \rrbracket\|_F^2 \\
 (4.26) \quad &\geq -C_1 \|\mathbf{u}_h\|_{V^c}^2 + C_2 \|p_h\|_{\Omega^\sharp}^2 - C_3 \sum_{K \in \mathcal{T}^\sharp} \|\mathfrak{p}^{-2} h_K \nabla p_h\|_K^2 - C_3 \sum_{F \in \mathcal{F}_{int}^\sharp} \|\mathfrak{p}^{-1} h_F^{1/2} \llbracket p_h \rrbracket\|_F^2,
 \end{aligned}$$

where  $C_1 = \frac{C_a}{2\lambda}$ ,  $C_2 = 1 - \frac{C_a + C_\sigma}{2} \lambda$  and  $C_3 = \frac{C_\sigma}{\lambda}$  are positive constants for small enough  $0 < \lambda < \frac{2}{C_a + C_\sigma}$ . Therefore, to gain the desired control and to balance the negative contribution  $\|\mathfrak{p}^{-4} h_K^2 \nabla p_h\|_K^2$  in (4.26), we test with  $(-\mathfrak{p}^{-4}\theta \nabla p_h, 0)$  using the continuity estimate (4.4) for  $\tilde{a}_h$ , the Cauchy-Schwarz inequality, the inverse estimate (3.4) and Young inequality. In particular,

$$\begin{aligned}
 A_h(\mathbf{u}_h, p_h; -\mathfrak{p}^{-4}\theta \nabla p_h, 0) &= \tilde{a}_h(\mathbf{u}_h, -\mathfrak{p}^{-4}\theta \nabla p_h) + b_h(-\mathfrak{p}^{-4}\theta \nabla p_h, p_h) \\
 &\geq -|\tilde{a}_h(\mathbf{u}_h, -\mathfrak{p}^{-4}\theta \nabla p_h)| - \sum_{K \in \mathcal{T}^\sharp} \|\mathfrak{p}^{-2} \theta^{1/2} \nabla p_h\|_K^2 + \sum_{F \in \mathcal{F}_{int}^\sharp} \int_F \{\mathfrak{p}^{-4}\theta \nabla p_h\} \cdot \mathbf{n}_F \llbracket p_h \rrbracket d\gamma \\
 &\geq -C_a \|\mathbf{u}_h\|_{V^c} \|\mathfrak{p}^{-4}\theta \nabla p_h\|_{V^c} - \sum_{K \in \mathcal{T}^\sharp} \|\mathfrak{p}^{-2} \theta^{1/2} \nabla p_h\|_K^2 \\
 &\quad + \widehat{C} \left( \sum_{F \in \mathcal{F}_{int}^\sharp} \|\mathfrak{p}^{-3} \theta^{3/4} \nabla p_h \cdot \mathbf{n}_F\|_F^2 \right)^{1/2} \left( \sum_{F \in \mathcal{F}_{int}^\sharp} \|\mathfrak{p}^{-1} \theta^{1/4} \llbracket p_h \rrbracket\|_F^2 \right)^{1/2}
 \end{aligned}$$

and we conclude to

$$\begin{aligned}
A_h(\mathbf{u}_h, p_h; -\mathfrak{p}^{-4}\theta \nabla p_h, 0) &\geq -\frac{C_a}{2\lambda_1} \|\mathbf{u}_h\|_{V^c}^2 - \frac{C_a \lambda_1}{2} \|\mathfrak{p}^{-4}\theta \nabla p_h\|_{V^c}^2 - \sum_{K \in \mathcal{T}^\sharp} \left\| \mathfrak{p}^{-2}\theta^{1/2} \nabla p_h \right\|_K^2 \\
&\quad + C \left( \sum_{K \in \mathcal{T}^\sharp} \|\mathfrak{p}^{-2}\theta^{3/4} h_K^{-1/2} \nabla p_h\|_K^2 \right)^{1/2} \left( \sum_{F \in \mathcal{F}_{int}^\sharp} \|\mathfrak{p}^{-1}\theta^{1/4} \llbracket p_h \rrbracket\|_F^2 \right)^{1/2} \\
&\stackrel{(4.28), \theta = h_K^2}{\geq} -\frac{C_a}{2\lambda_1} \|\mathbf{u}_h\|_{V^c}^2 - \frac{\tilde{C} C_a \lambda_1}{2} \sum_{\mathcal{K} \in \mathcal{T}^{cov}} \|\mathfrak{p}^{-2} h_K \nabla p_h\|_{\mathcal{K}}^2 - \sum_{K \in \mathcal{T}^\sharp} \|\mathfrak{p}^{-2} h_K \nabla p_h\|_K^2 \\
&\quad + \frac{C \lambda_2}{2} \sum_{K \in \mathcal{T}^\sharp} \|\mathfrak{p}^{-2} h_K \nabla p_h\|_K^2 + \frac{C}{2\lambda_2} \sum_{F \in \mathcal{F}_{int}^\sharp} \left\| \mathfrak{p}^{-1} h_F^{1/2} \llbracket p_h \rrbracket \right\|_F^2 \\
&\geq -\frac{C_a}{2\lambda_1} \|\mathbf{u}_h\|_{V^c}^2 - \sum_{K \in \mathcal{T}^\sharp} \|\mathfrak{p}^{-2} h_K \nabla p_h\|_K^2 - \frac{C_p}{2} (\tilde{C} C_a \lambda_1 - C \lambda_2) \|\mathfrak{p}^{-2} h_K \nabla p_h\|_{\Omega^\sharp}^2 \\
&\quad + \frac{C}{2\lambda_2} \sum_{F \in \mathcal{F}_{int}^\sharp} \left\| \mathfrak{p}^{-1} h_F^{1/2} \llbracket p_h \rrbracket \right\|_F^2 \\
(4.27) \quad &\geq -C_4 \|\mathbf{u}_h\|_{V^c}^2 + C_5 \sum_{K \in \mathcal{T}^\sharp} \|\mathfrak{p}^{-2} h_K \nabla p_h\|_K^2 + C_6 \sum_{F \in \mathcal{F}_{int}^\sharp} \left\| \mathfrak{p}^{-1} h_F^{1/2} \llbracket p_h \rrbracket \right\|_F^2
\end{aligned}$$

where  $C_4 = \frac{C_a}{2\lambda_1}$ ,  $C_5 = 1 - \frac{C_p}{2} (\tilde{C} C_a \lambda_1 - C \lambda_2)$  and  $C_6 = \frac{C}{2\lambda_2}$  are positive constants for properly chosen  $\lambda_1 > 2/(c_p \tilde{C} C_a) > 0$  and  $0 < \lambda_2 < 2/(c_p C) (c_p \tilde{C} C_a \lambda_1/2 - 1)$ .

We note that in the last inequality  $\tilde{C} > 0$ , we take  $\sigma = \mathfrak{p} h_K^{-1/2}$  and we derive the bound

$$\begin{aligned}
\|\mathfrak{p}^{-4}\theta \nabla p_h\|_{V^c}^2 &= \|\mathfrak{p}^{-4}\theta \nabla \nabla p_h\|_{\Omega^{cov}}^2 + \sum_{F \in \mathcal{T}^\sharp \cap \Gamma} \left\| \mathfrak{p}^{-3}\theta h_F^{-1/2} \nabla p_h \right\|_F^2 + \sum_{F \in \mathcal{F}_{int}^\sharp} \left\| \mathfrak{p}^{-3}\theta h_F^{-1/2} \llbracket \nabla p_h \rrbracket \right\|_F^2 \\
&\leq \sum_{\mathcal{K} \in \mathcal{T}^{cov}} \|\mathfrak{p}^{-2}\theta h_K^{-1} \nabla p_h\|_{\mathcal{K}}^2 + \sum_{F \in \mathcal{T}^\sharp \cap \Gamma} \left\| \mathfrak{p}^{-3}\theta h_F^{-1/2} \nabla p_h \right\|_F^2 + \sum_{F \in \mathcal{F}_{int}^\sharp} \left\| \mathfrak{p}^{-3}\theta h_F^{-1/2} \llbracket \nabla p_h \rrbracket \right\|_F^2 \\
(4.28) \quad &\leq \tilde{C} \sum_{\mathcal{K} \in \mathcal{T}^{cov}} \|\mathfrak{p}^{-2} h_K \nabla p_h\|_{\mathcal{K}}^2
\end{aligned}$$

which has been obtained by the trace inequalities (3.4), the inverse inequality (3.7) and finally setting  $\theta = h_K^2$ . In particular, if we regard the norm on a facet  $F \subset \partial K \in \mathcal{T}^\sharp$ ,

$$\|\sigma \mathfrak{p}^{-4} h_F^2 \nabla p_h\|_F \leq \left\| \mathfrak{p}^{-3} h_F^{3/2} \nabla p_h \right\|_F \leq \left\| \mathfrak{p}^{-3} h_F^{3/2} \nabla p_h \right\|_{\partial K} \leq C \mathfrak{p}^{-2} h_K \|\nabla p_h\|_K,$$

by (3.4) and (3.7) respectively. Then, the norm corresponding to the jump on  $F = K \cap K'$  satisfies  $\left\| \mathfrak{p}^{-3} h_F^{3/2} \llbracket \nabla p_h \rrbracket \right\|_F \leq C \mathfrak{p}^{-2} h_K \max \{ \|\nabla p_h\|_K, \|\nabla p_h\|_{K'} \}$  leading to the estimate

$$\sum_{F \in \mathcal{F}_{int}^\sharp} \left\| \mathfrak{p}^{-3} h_F^{3/2} \llbracket \nabla p_h \rrbracket \right\|_F^2 \leq C \sum_{K \in \mathcal{T}^\sharp} \|\mathfrak{p}^{-2} h_K \nabla p_h\|_K^2.$$

Proceeding in a similar way for the other terms, we obtain (4.28).

Finally, we collect inequalities (4.25)–(4.27) and we choose  $(\mathbf{v}_h, q_h) = (\mathbf{u}_h, -p_h) + \zeta_1(-\mathbf{w}_h, 0) + \zeta_2(-\mathfrak{p}^{-4}h_K^2 \nabla p_h, 0)$ . Then, we obtain that

$$\begin{aligned}
& A_h(\mathbf{u}_h, p_h; \mathbf{v}_h, q_h) \geq c_a \|\mathbf{u}_h\|_{V^c}^2 \\
& + \zeta_1(-C_1 \|\mathbf{u}_h\|_{V^c}^2 + C_2 \|p_h\|_{\Omega^\sharp}^2 - C_3 \sum_{K \in \mathcal{T}^\sharp} \|\mathfrak{p}^{-2} h_K \nabla p_h\|_K^2 - C_3 \sum_{F \in \mathcal{F}_{int}^\sharp} \|\mathfrak{p}^{-1} h_F^{1/2} [p_h]\|_F^2) \\
& \quad \zeta_2(-C_4 \|\mathbf{u}_h\|_{V^c}^2 + C_5 \sum_{K \in \mathcal{T}^\sharp} \|\mathfrak{p}^{-2} h_K \nabla p_h\|_K^2 + C_6 \sum_{F \in \mathcal{F}_{int}^\sharp} \|\mathfrak{p}^{-1} h_F^{1/2} [p_h]\|_F^2) \\
& \geq (c_a - \zeta_1 C_1 - \zeta_2 C_4) \|\mathbf{u}_h\|_{V^c}^2 + \zeta_1 C_2 \|p_h\|_{\Omega^\sharp}^2 + (\zeta_2 C_5 - \zeta_1 C_3) \sum_{K \in \mathcal{T}^\sharp} \|\mathfrak{p}^{-2} h_K \nabla p_h\|_K^2 \\
& \quad + (\zeta_2 C_6 - \zeta_1 C_3) \sum_{F \in \mathcal{F}_{int}^\sharp} \|\mathfrak{p}^{-1} h_F^{1/2} [p_h]\|_F^2. \tag{4.29}
\end{aligned}$$

We force  $\zeta_1 \leq C_3^{-1} \min\{C_5, C_6\} \zeta_2$  or  $\zeta_2 \geq C_3 \min\{C_5, C_6\}^{-1} \zeta_1$  and we choose  $\zeta_2 = 2C_3 \min\{C_5, C_6\}^{-1} \zeta_1$ . We finally impose  $\zeta_1 \leq c_a / (C_1 + 2C_3 \min\{C_5, C_6\}^{-1})$  and we conclude that

$$A_h(\mathbf{u}_h, p_h; \mathbf{v}_h, q_h) \leq C(\|\mathbf{u}_h\|_{V^c}^2 + \|p_h\|_{Q^c}^2) = C\|(\mathbf{u}_h, p_h)\|_{V^c, Q^c}^2, \text{ for } C > 0.$$

We now note that

$$\begin{aligned}
\|(\mathbf{u}_h - \zeta_1 \mathbf{w}_h - \zeta_2 \mathfrak{p}^{-4} h_K^2 \nabla p_h, -p_h)\|_{V^c, Q^c}^2 &= \|\mathbf{u}_h - \zeta_1 \mathbf{w}_h - \zeta_2 \mathfrak{p}^{-4} h_K^2 \nabla p_h\|_{V^c}^2 + \|p_h\|_{Q^c}^2 \\
&\leq \|\mathbf{u}_h\|_{V^c}^2 + \zeta_1 \|\mathbf{w}_h\|_{V^c}^2 + \zeta_2 \|\mathfrak{p}^{-4} h_K^2 \nabla p_h\|_{V^c}^2 + \|p_h\|_{Q^c}^2 \\
&\leq \|\mathbf{u}_h\|_{V^c}^2 + (\zeta_1 + 2C_3 \min\{C_5, C_6\}^{-1} \zeta_1 + 1) \|p_h\|_{Q^c}^2 \\
&\leq ((\zeta_1(1 + 2C_3 \min\{C_5, C_6\}^{-1}) + 1) \|(\mathbf{u}_h, p_h)\|_{V^c, Q^c}^2,
\end{aligned}$$

and the proof of (4.24) follows, where  $c_{bil} = \frac{\min\{c_a - \zeta_1(C_1 + 2C_3 \min\{C_5, C_6\}^{-1})C_4, \zeta_1 C_2\}}{\zeta_1(1 + 2C_3 \min\{C_5, C_6\}^{-1}) + 1}$ .  $\square$

## 5. ERROR ESTIMATES

Next, we introduce the asymptotic Galerkin orthogonality and consistency of the variational formulation (2.6). To obtain error estimates, in this section we will assume that the exact solution  $(\mathbf{u}, p) \in [H_0^1(\Omega^\sharp)]^d \times L_0^2(\Omega^\sharp)$ .

**Lemma 5.1.** *Let  $(\mathbf{u}, p) \in [H^2(\Omega^\sharp) \cap H_0^1(\Omega^\sharp)]^d \times [H^1(\Omega^\sharp) \cap L_0^2(\Omega^\sharp)]$  be the solution to the Stokes problem (2.1) and  $(\mathbf{u}_h, p_h) \in V_h^\sharp \times Q_h^\sharp$  the finite element approximation in (2.6), with  $h = \max_{K \in \mathcal{T}^{cov}} h_K$  due to shape regularity of  $\mathcal{T}^{cov}$ , see also Assumption 3.9. Then,*

$$(5.1) \quad A_h(\mathbf{u} - \mathbf{u}_h, p - p_h; \mathbf{v}_h, q_h) = \mathcal{O}(h^\mathfrak{p} / \mathfrak{p}^{\mathfrak{p} - \frac{1}{2}}) \quad \text{for every } (\mathbf{v}_h, q_h) \in V_h^\sharp \times Q_h^\sharp.$$

Next we prove the a priori error estimate and optimal convergence rates for the velocity and pressure.

**Theorem 5.2.** *Let  $(\mathbf{u}, p) \in [H^{\mathfrak{p}+1}(\Omega^\sharp) \cap H_0^1(\Omega^\sharp)]^d \times [H^\mathfrak{p}(\Omega^\sharp) \cap L_0^2(\Omega^\sharp)]$  be the solution to the Stokes problem (2.1) and  $(\mathbf{u}_h, p_h) \in V_h^\sharp \times Q_h^\sharp$  the finite element approximation in agreement with (2.6). Then, there exists a constant  $C > 0$ , such that*

$$(5.2) \quad \|(\mathbf{u} - \mathbf{u}_h, p - p_h)\| \leq C \sum_{K \in \mathcal{T}^\sharp} \frac{h_K^\mathfrak{p}}{\mathfrak{p}^{\mathfrak{p} - \frac{1}{2}}} \left( \|\mathbf{u}\|_{\mathfrak{p}+1, K} + \frac{1}{\mathfrak{p}^{\frac{1}{2}}} \|p\|_{\mathfrak{p}, K} \right).$$

*Proof.* We start by rearranging the  $(\mathbf{u} - \mathbf{u}_h, p - p_h)$  error adding and subtracting appropriate terms, and we conclude to its discrete and projection error components:

$$\|(\mathbf{u} - \mathbf{u}_h, p - p_h)\| \leq \|(\mathbf{u} - \Pi_h \mathbf{u}, p - \Pi_h p)\| + \|(\Pi_h \mathbf{u} - \mathbf{u}_h, \Pi_h p - p_h)\|.$$

The first term optimal estimate is provided by (4.13) and (4.14) as it is proven in Corollary 4.4. The second term, first is bounded by

$$\|(\Pi_h \mathbf{u} - \mathbf{u}_h, \Pi_h p - p_h)\| \leq C \|(\Pi_h \mathbf{u} - \mathbf{u}_h, \Pi_h p - p_h)\|_{V^c, Q^c},$$

according to (3.2). Due to (5.1) from Lemma 5.1 and Theorem 4.7 there exists a pair  $(\mathbf{v}_h, q_h) \in V_h^\sharp \times Q_h^\sharp$  with  $\|(\mathbf{v}_h, q_h)\|_{V^c, Q^c} = 1$ , such that

$$c_{bil} \|(\Pi_h \mathbf{u} - \mathbf{u}_h, \Pi_h p - p_h)\|_{V^c, Q^c} \leq A_h(\Pi_h \mathbf{u} - \mathbf{u}_h, \Pi_h p - p_h; \mathbf{v}_h, q_h) = A_h(\Pi_h \mathbf{u} - \mathbf{u}, \Pi_h p - p; \mathbf{v}_h, q_h).$$

Hence, we use the definition of the corresponding form  $A_h$  to take

$$(5.3) \quad A_h(\Pi_h \mathbf{u} - \mathbf{u}, \Pi_h p - p; \mathbf{v}_h, q_h) = \tilde{a}_h(\Pi_h \mathbf{u} - \mathbf{u}, \mathbf{v}_h) + b_h(\mathbf{v}_h, \Pi_h p - p) + b_h(\Pi_h \mathbf{u} - \mathbf{u}, q_h).$$

Next, recalling that the pair  $(\mathbf{v}_h, q_h)$  has unit  $\|\cdot\|_{V^c, Q^c}$  norm, we derive

$$A_h(\Pi_h \mathbf{u} - \mathbf{u}, \Pi_h p - p; \mathbf{v}_h, q_h) \leq C_a \|\Pi_h \mathbf{u} - \mathbf{u}\| \cdot \|v_h\| + C_b \|v_h\| \cdot \|\Pi_h p - p_h\| + C_b \|\Pi_h \mathbf{u} - \mathbf{u}\| \cdot \|q_h\|,$$

after employing the continuity of  $\tilde{a}_h$  and  $b_h$  in (4.5)–(4.7) and Corollary 4.4, also bounds the remaining terms. At this end, an estimate for (5.3) follows as

$$\begin{aligned} A_h(\Pi_h \mathbf{u} - \mathbf{u}, \Pi_h p - p; \mathbf{v}_h, q_h) &\leq C \sum_{K \in \mathcal{T}^\sharp} \frac{h_K^\sharp}{\mathfrak{p}^{\mathfrak{p}-\frac{1}{2}}} \left\{ \max \{ \|v_h\| \cdot \|q_h\| \} \left( 3\|\mathbf{u}\|_{\mathfrak{p}+1, K} + \frac{1}{\mathfrak{p}^{\frac{1}{2}}} \|p\|_{\mathfrak{p}, K} \right) \right\} \\ &\leq C \sum_{K \in \mathcal{T}^\sharp} \frac{h_K^\sharp}{\mathfrak{p}^{\mathfrak{p}-\frac{1}{2}}} \left( \|\mathbf{u}\|_{\mathfrak{p}+1, K} + \frac{1}{\mathfrak{p}^{\frac{1}{2}}} \|p\|_{\mathfrak{p}, K} \right), \end{aligned}$$

and the estimate (5.2) follows.  $\square$

*Remark 5.3.* We note that if one makes stronger assumptions as mesh quasi-uniformity:  $h = \max_{K \in \mathcal{T}^\sharp} h_K$ , then the estimate of Theorem 5.2 is transformed to  $\|(\mathbf{u} - \mathbf{u}_h, p - p_h)\| \leq C \frac{h^\sharp}{\mathfrak{p}^{\mathfrak{p}-\frac{1}{2}}} \left( \|\mathbf{u}\|_{\mathfrak{p}+1, \Omega^\sharp} + \frac{1}{\mathfrak{p}^{\frac{1}{2}}} \|p\|_{\mathfrak{p}, \Omega^\sharp} \right)$ , which verifies optimal convergence in  $h$  and suboptimal in  $p$  by  $p^{1/2}$ .

## 6. NUMERICAL EXPERIMENTS/CONVERGENCE TESTS

We consider a two-dimensional test case of (2.1) in the unit square  $\Omega^\sharp = [0, 1]^2$  with exact solution

$$\mathbf{u}(x, y) = (u(x, y), -u(y, x)), \quad p(x, y) = \sin(2\pi x) \cos(2\pi y),$$

where  $u(x, y) = (\cos(2\pi x) - 1) \sin(2\pi y)$ . Note that the mean value of  $p(x, y)$  over  $\Omega^\sharp$  vanishes by construction, thus ensuring that the problem (2.1) is uniquely solvable. As in subsection 2.2, in the spirit of a fictitious domain approach, we consider the original domain  $\Omega^\sharp$  as being immersed in the background domain  $\Omega = [-0.5, 1.5]^2$  (see Figure 2). A level set description of the geometry is possible through the function

$$(6.1) \quad \phi(x, y) = |x - 0.5| + |y - 0.5| + |x - 0.5| - |y - 0.5| - 1 < 0.$$

To investigate error convergence behavior of the discretization (2.6), we consider a sequence of successively refined tessellations  $\{\mathcal{T}_{h_i}^\sharp\}_{i>0}$  of  $\Omega^\sharp$  with mesh parameters  $h_i = 2^{-i-2}$ , for  $i = 0, \dots, 7$ . As it is shown in Figure 2, exploiting the level-set function information on  $\partial\Omega^\sharp$ , elements containing straight faces approximating the curved boundary are marked. Finally, all marked elements are treated as curved triangular elements with two straight faces and one curved face described by the domain level-set function, thus capturing the domain exactly. To allow for several polynomial degrees  $\mathfrak{p}_i$ , the symmetric interior penalty parameter in (2.4) scales as  $\sigma = \mathfrak{p}_i^2/h_i$ . A sparse direct solver has been used to solve the arising linear systems.

As expected from the theoretical error estimate stated in Theorem 5.2, optimal  $\mathfrak{p}$ -th order convergence rates with respect to the  $H^1$ -norm of the velocity error and the  $L^2$ -norm of the pressure error are in agreement with the error results as they are visualized in Table 1 ( $\mathfrak{p} = 1$ ), Table 2 ( $\mathfrak{p} = 2$ ) for both velocity and pressure and in Table 3 ( $\mathfrak{p} = 3$ ) optimal for velocity and suboptimal for pressure. The superiority of the higher order framework is obvious and show that the method is efficient. Numerical experiments verify these facts, indeed, for larger  $\mathfrak{p}$ , much smaller errors are attained in progressively coarser meshes, for  $\mathfrak{p}_i/\mathfrak{p}_{i-1}$  Taylor–Hood velocity/pressure pairs order, and the inf–sup stability is guaranteed. Further investigation, revealed that contrasting the results between Table 3 and Table 4 related to the  $\mathfrak{p}_3/\mathfrak{p}_2$  case, i.e. comparing the suggested in the present work framework with no stabilization on the boundary zone area, against to the full ghost penalty stabilization, showed that: the method as suggested in the present work, yields better error behavior and similar convergence rates with the stabilized one. Therefore, we avoided integration errors related to the normal derivative up to the third-order jump terms, [43, 44], which lead to a significant improvement in the velocity and pressure errors, as well as, crucial computational cost savings.

Discretization		Errors and convergence rates: $p_1/p_0$ polynomials case			
$h_{\max}$		$\ \mathbf{u} - \mathbf{u}_h\ _{1,\Omega^\sharp}$	Conv. rate	$\ p - p_h\ _{\Omega^\sharp}$	Conv. rate
0.25( $= 2^{-2}$ )		1.469461	—	0.8756151	—
0.125( $= 2^{-3}$ )		0.871741	0.7533148	0.4336638	1.0137197
0.0625( $= 2^{-4}$ )		0.526300	0.7280155	0.3289021	0.3989189
0.03125( $= 2^{-5}$ )		0.290011	0.8597764	0.1901614	0.7904334
0.015625( $= 2^{-6}$ )		0.151577	0.9360504	0.1006410	0.9180059
0.0078125( $= 2^{-7}$ )		0.077476	0.9682347	0.0515098	0.9662987
0.00390625( $= 2^{-8}$ )		0.039269	0.9803399	0.0261353	0.9788479
Mean:		—	0.8709553	—	0.8443707

TABLE 1. Errors and rates of convergence with respect to  $H^1$ -norm for the velocity and  $L^2$ -norm for the pressure, using  $p_1/p_0$  finite elements without boundary elements area stabilization.

Discretization		Errors and convergence rates: $p_2/p_1$ polynomials case			
$h_{\max}$		$\ \mathbf{u} - \mathbf{u}_h\ _{1,\Omega^\sharp}$	Conv. rate	$\ p - p_h\ _{\Omega^\sharp}$	Conv. rate
0.25( $= 2^{-2}$ )		0.2372591	—	0.1131108	—
0.125( $= 2^{-3}$ )		0.1129321	1.0710074	0.0512201	1.1429531
0.0625( $= 2^{-4}$ )		0.0337229	1.7436526	0.0165609	1.6289302
0.03125( $= 2^{-5}$ )		0.0088867	1.9240082	0.0046825	1.8224281
0.015625( $= 2^{-6}$ )		0.0023107	1.9433135	0.0012434	1.9129403
0.0078125( $= 2^{-7}$ )		0.0005816	1.9900301	0.0003073	2.0165782
Mean:		—	1.7344024	—	1.7047660

TABLE 2. Errors and rates of convergence with respect to  $H^1$ -norm for the velocity and  $L^2$ -norm for the pressure, using  $p_2/p_1$  and finite elements without boundary elements area stabilization.

Discretization		Errors and convergence rates: $p_3/p_2$ polynomials case			
$h_{\max}$		$\ \mathbf{u} - \mathbf{u}_h\ _{1,\Omega^\sharp}$	Conv. rate	$\ p - p_h\ _{\Omega^\sharp}$	Conv. rate
0.25( $= 2^{-2}$ )		0.0466716	—	0.0184400	—
0.125( $= 2^{-3}$ )		0.0076981	2.5999546	0.0069364	1.4105717
0.0625( $= 2^{-4}$ )		0.0012099	2.6696092	0.0017273	2.0056609
0.03125( $= 2^{-5}$ )		0.0001644	2.8789030	0.0009789	0.8192784
0.015625( $= 2^{-6}$ )		2.5518e-05	2.6883086	0.0003071	1.6720465
Mean:		—	2.7091938	—	1.4768894

TABLE 3. Errors and rates of convergence with respect to  $H^1$ -norm for the velocity and  $L^2$ -norm for the pressure, using  $p_3/p_2$  finite elements without boundary elements area stabilization.

It is important to underline that the evaluation of boundary elements stabilization is avoided, namely, computations of gradually higher order normal derivative jumps –depended on the finite element order– seem unnecessary with the suggested approach. Finally, in Figure 4, a sequence of approximations for the velocity and pressure solution in progressively finer meshes and polynomial degrees in a  $hp$  sense are illustrated, showcasing the efficient convergence of the method and the robustness of the errors with respect to several orders of  $hp$  consideration in all three polynomial order cases. We highlight that the pressure convergence rate in Table 3 is suboptimal although the error is much smaller e.g. than the case where full boundary area elements stabilization is applied in the  $p_3/p_2$  as it is reported in Table 4.

Discretization		Errors and convergence rates: $p_3/p_2$ polynomials case			
$h_{\max}$		$\ \mathbf{u} - \mathbf{u}_h\ _{1,\Omega^\sharp}$	Conv. rate	$\ p - p_h\ _{\Omega^\sharp}$	Conv. rate
0.25( $= 2^{-2}$ )		0.3386166	—	0.7184173	—
0.125( $= 2^{-3}$ )		0.0247465	3.7743523	0.0590158	3.60564722
0.0625( $= 2^{-4}$ )		0.0039329	2.6535468	0.0096287	2.61568216
0.03125( $= 2^{-5}$ )		0.0006434	2.6117326	0.0017089	2.4942619
0.015625( $= 2^{-6}$ )		0.0002045	1.6536038	0.0003671	2.2187371
Mean:		—	2.67330889	—	2.73358212

TABLE 4. Errors and rates of convergence with respect to  $H^1$ -norm for the velocity and  $L^2$ -norm for the pressure, using  $p_3/p_2$  finite elements with full boundary elements area stabilization.

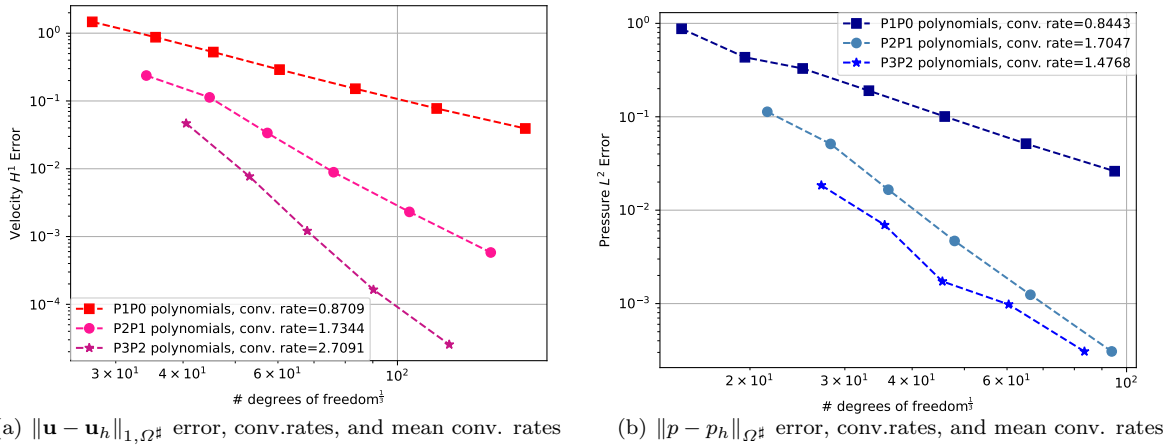


FIGURE 4. Visualization of the  $H^1$ -norm velocity errors and  $L^2$ -norm pressure errors with respect to the discretization size.

*Remark 6.1.* We note that in practice, the condition number for arbitrarily shaped boundary elements discontinuous Galerkin methods to solve Stokes problem is typically very large. The employment of efficient multigrid preconditioners for such cases, is left as a further challenge, see also the works [1], [22]. We also clarify that for the curved boundary elements, the current implementation performs quadrature by a sufficiently fine sub-triangulation approximating properly the curved element. It is noted that in this case the sub-triangulation is only used to generate the quadrature rules. Of course, this is not the only possibility. For instance, domain-exact quadrature algorithms for many curved domains exist, for such algorithms see [3, 23] and the references therein.

## 7. CONCLUSION

In this effort, we proposed and tested an unstabilized boundary element interface discontinuous Galerkin method for the incompressible Stokes flow. Optimal order convergence is proved for higher order finite elements of  $p_i/p_{i-1}$  order for velocity and pressure fields. This method may prove valuable in applications where special emphasis is placed on the effective approximation of pressure, attaining much smaller relative errors in coarser meshes. In fact, control over the error of the pressure field is among the most decisive points of difficulty for many methods. Numerical test experiments demonstrated the very good stability and accuracy properties of the method. The theoretical convergence rates for the  $H^1$ -norm of the velocity and the  $L^2$ -norm of the pressure have been validated by our tests, even for the  $p_3/p_2$  case. Finally, the numerical experiments indicated that the values of the symmetric interior penalty parameter  $\sigma$  should be carefully selected to ensure stability and accuracy

in the case of higher order finite elements. In the present work, we focused on the static Stokes problem. Future work will extend our investigations to more general fluid mechanics problems, including time-dependent problems on complex domains and/or nonlinearities.

#### ACKNOWLEDGMENTS

This project has received funding from “First Call for H.F.R.I. Research Projects to support Faculty members and Researchers and the procurement of high-cost research equipment” grant 3270 and was supported by computational time granted from the National Infrastructures for Research and Technology S.A. (GRNET S.A.) in the National HPC facility - ARIS - under project ID pa190902. The author would like also to thank Prof. Emmanuil Georgoulis from NTUA for valuable comments and inspiring ideas. We would like also to thank the contributors of the ngsolve-ngsxfem, [40, 54].

#### REFERENCES

1. A. Aretaki and E. N. Karatzas, *Random geometries for optimal control PDE problems based on fictitious domain FEMs and cut elements*, Journal of Computational and Applied Mathematics **412** (2022), 114286.
2. A. Aretaki, E. N. Karatzas, and G. Katsouleas, *Equal Higher Order Analysis of an Unfitted Discontinuous Galerkin Method for Stokes Flow Systems*, J. Sci. Comput. **91** (2022), no. 2, 48.
3. E. Artioli, A. Sommariva, and M. Vianello, *Algebraic cubature on polygonal elements with a circular edge*, Computers & Mathematics with Applications **79** (2020), no. 7, 2057–2066, Advanced Computational methods for PDEs.
4. A. Baker, W. N. Jureidini, and O. A. Karakashian, *Piecewise solenoidal vector fields and the Stokes problem*, SIAM J. Numer. Anal. **27** (1990), 1466–1485.
5. J. W. Barrett and C. M. Elliott, *Fitted and Unfitted Finite-Element Methods for Elliptic Equations with Smooth Interfaces*, IMA Journal of Numerical Analysis **7** (1987), no. 3, 283–300.
6. P. Bastian and C. Engwer, *An unfitted finite element method using discontinuous Galerkin*, J. Numer. Meth. Engrg. **79** (2009), 1557–1576.
7. P. Bastian, C. Engwer, J. Fahlke, and O. Ippisch, *An unfitted discontinuous galerkin method for pore-scale simulations of solute transport*, Math. Comput. Simulat. **81** (2011), 2051–2061.
8. L. Beirao Da Veiga, F. Brezzi, A. Cangiani, G. Manzini, L. D. Marini, and A. Russo, *Basic principles of virtual element methods*, Mathematical Models and Methods in Applied Sciences **23** (2013), no. 01, 199–214.
9. L. Beirao Da Veiga, K. Lipnikov, and G. Manzini, *The mimetic finite difference method for elliptic problems*, MS&A Modeling, Simulation and Applications Springer, Cham, 2014.
10. W. Bo and J. W. Grove, *volume of fluid method based ghost fluid method for compressible multi-fluid flows*, Computers & Fluids **90** (2014), 113–122.
11. E. Burman and P. Hansbo, *Fictitious domain finite element methods using cut elements II*, A stabilized Nitsche method, Appl. Num. Math. **62** (2012), no. 4, 328–341.
12. ———, *Fictitious domain methods using cut elements: III. A stabilized Nitsche method for Stokes problem*, ESAIM: Math. Model. Numer. Anal. 48(3), 859–874 (2014) **48** (2014), no. 3, 859–874.
13. A. Cangiani, Z. Dong, and E. H. Georgoulis, *hp-Version discontinuous Galerkin methods on essentially arbitrarily-shaped elements*, Math. Comput. **91** (2022), 1–35.
14. A. Cangiani, Z. Dong, E. H. Georgoulis, and P. Houston, *hp-Version discontinuous Galerkin methods for advection-diffusion-reaction problems on polytopic meshes*, ESAIM: M2AN **50** (2016), no. 3, 699–725.
15. A. Cangiani, Z. Dong, E.H. Georgoulis, and P. Houston, *hp-Version Discontinuous Galerkin Methods on Polygonal and Polyhedral Meshes*, SpringerBriefs in Mathematics, Springer International Publishing, 2017.
16. A. Cangiani, E. H. Georgoulis, and Y. A. Sabawi, *Adaptive discontinuous Galerkin methods for elliptic interface problems*, Math. Comput. **87** (2018), 2675–2707.
17. B. Cockburn, J. Gopalakrishnan, and R. Lazarov, *Unified Hybridization of Discontinuous Galerkin, Mixed, and Continuous Galerkin Methods for Second Order Elliptic Problems*, SIAM Journal on Numerical Analysis **47** (2009), no. 2, 1319–1365.
18. B. Cockburn, G. Kanschat, D. Schötzau, and C. Schwab, *Local discontinuous Galerkin methods for the Stokes system*, SIAM J. Numer. Anal **40** (2002), 319–343.
19. D. A. Di Pietro and A. Ern, *Mathematical aspects of discontinuous Galerkin methods*, vol. 69, Springer, 2012.
20. ———, *A hybrid high-order locking-free method for linear elasticity on general meshes*, Computer Methods in Applied Mechanics and Engineering **283** (2015), 1–21.
21. H. Dong, B. Wang, Z. Xie, and L. Wang, *An unfitted hybridizable discontinuous Galerkin method for the Poisson interface problem and its error analysis*, IMA J. Numer. Anal. **37** (2016), 444–476.
22. Z. Dong, *Discontinuous galerkin methods for the biharmonic problem on polygonal and polyhedral meshes*, International Journal of Numerical Analysis and Modeling **Volume 16** (2019), 825–846.
23. Z. Dong, E. H. Georgoulis, and Kapas T., *GPU-accelerated discontinuous Galerkin methods on polytopic meshes*, SIAM J. Sci. Comput. **43** (2021), C312–C334.
24. Z. Dong and L. Mascotto, *hp-optimal interior penalty discontinuous Galerkin methods for the biharmonic problem*, arXiv preprint arXiv:2212.03735 (2022).
25. M. Duprez and A. Lozinski,  *$\phi$ -fem a finite element method on domains defined by level-sets*, (2019), arXiv: 1901.03966v3.
26. C. Engwer, S. May, A. Nüßing, and F. Streitbürger, *A Stabilized DG Cut Cell Method for Discretizing the Linear Transport Equation*, SIAM Journal on Scientific Computing **42** (2020), no. 6, A3677–A3703.

27. C. Engwer, T. Ranner, and S. Westerheide, *An unfitted discontinuous Galerkin scheme for conservation laws on evolving surfaces*, Proceedings of the Conference Algoritmy (2016), 44–54.
28. T. Fries and T. Belytschko, *The extended/generalized finite element method: An overview of the method and its applications*, International Journal for Numerical Methods in Engineering **84** (2010), no. 3, 253–304.
29. E. H. Georgoulis, Edward J. C. Hall, and J. M. Melenk, *On the Suboptimality of the  $p$ -Version Interior Penalty Discontinuous Galerkin Method*, Journal of Scientific Computing **42** (2010), 54–67.
30. V. Girault, B. Rivière, and M. A. Wheeler, *Discontinuous Galerkin method with non-overlapping domain decomposition for the Stokes and Navier–Stokes problems*, Math. Comput. **74** (2005), 53–84.
31. A. Hansbo and P. Hansbo, *An unfitted finite element method, based on Nitsche’s method, for elliptic interface problems*, Comput. Methods Appl. Mech. Eng **191** (2002), 5537–5552.
32. Paul Houston et al., *Discontinuous  $hp$ -finite element methods for advection-diffusion-reaction problems*, SIAM Journal on Numerical Analysis **39** (2002), no. 6, 2133–2163.
33. L. N. T. Huynh, N. C. Nguyen, J. Peraire, and B. C. Khoo, *A high order hybrizidable discontinuous Galerkin method for elliptic interface problems*, Int. J. Numer. Meth. Engrg. **93** (2013), 183–200.
34. E. N. Karatzas, F. Ballarin, and G. Rozza, *Projection-based reduced order models for a cut finite element method in parametrized domains*, Computers & Mathematics with Applications **3** (2020), no. 79, 833–851.
35. E. N. Karatzas and G. Rozza, *A Reduced Order Model for a Stable Embedded Boundary Parametrized Cahn–Hilliard Phase-Field System Based on Cut Finite Elements*, J Sci Comput **89** (2021), no. 9.
36. E. N. Karatzas, G. Stabile, N. Atallah, G. Scovazzi, and G. Rozza, *A reduced order approach for the embedded shifted boundary fem and a heat exchange system on parametrized geometries*, IUTAM Symposium on Model Order Reduction of Coupled Systems, Stuttgart, Germany, May, 2018. IUTAM Bookseries, vol 36. Springer, Cham, 2020, pp. 22–25.
37. E. N. Karatzas, G. Stabile, L. Nouveau, G. Scovazzi, and G. Rozza, *A reduced basis approach for PDEs on parametrized geometries based on the shifted boundary finite element method and application to a Stokes flow*, Comput. Methods Appl. Mech. Engrg. **347** (2019), 568–587.
38. ———, *A reduced-order shifted boundary method for parametrized incompressible Navier–Stokes equations*, Comput. Methods Appl. Mech. Engrg. **370** (2020), 113–273.
39. E. M. Kolahdouz, A. P. S. Bhalla, B. A. Craven, and B. E. Griffith, *An immersed interface method for faceted surfaces*, Journal of Computational Physics **400** (2020).
40. C. Lehrenfeld, F. Heimann, J. Preuß, and H. von Wahl, *ngsxfem: Add-on to ngsolve for geometrically unfitted finite element discretizations*, Journal of Open Source Software **6** (2021), no. 64, 32–37.
41. A. Lozinski, *Cutfem without cutting the mesh cells: a new way to impose dirichlet and neumann boundary conditions on unfitted meshes*, Computer Methods in Applied Mechanics and Engineering **356** (2019), 75–100.
42. A. Main and G. Scovazzi, *The shifted boundary method for embedded domain computations. Part I: Poisson and Stokes problems*, Journal of Computational Physics **372** (2018), 972–995.
43. A. Massing, M. G. Larson, A. Logg, and M. E. Rognes, *A stabilized Nitsche fictitious domain method for the Stokes problem*, J. Sci. Comput. **61** (2014), 604–628.
44. ———, *A stabilized Nitsche overlapping mesh method for the Stokes problem*, Numer. Math. **128** (2014), 73–101.
45. R. Massjung, *An unfitted discontinuous galerkin method applied to elliptic interface problems*, SIAM J. Numer. Anal. **50** (2012), 3134–3162.
46. J. M. Melenk, *hp-finite element methods for singular perturbations*, 2002.
47. V. Murti and S. Valliappan, *Numerical inverse isoparametric mapping in remeshing and nodal quantity contouring*, Computers & Structures **22** (1986), no. 6, 1011–1021.
48. V. Murti, Y. Wang, and S. Valliappan, *Numerical inverse isoparametric mapping in 3D FEM*, Computers & Structures **29** (1988), no. 4, 611–622.
49. S. J. Osher and R. Fedkiw, *Level set methods and dynamic implicit surfaces*, Applied mathematical sciences, vol. 153, Springer, 2003.
50. V. Pasquariello, F. Hammerl, G. Örley, S. Hickel, C. Danowski, A. Popp, W.A. Wall, and N.A. Adams, *A cut-cell finite volume–finite element coupling approach for fluid–structure interaction in compressible flow*, J. Comput. Phys. **307** (2016), 670–695.
51. C. S. Peskin, *Flow patterns around heart valves: A numerical method*, J. Comput. Phys. **10** (1972), 252–271.
52. D. Schötzau, C. Schwab, and A. Toselli, *Mixed  $hp$ -DGFEM for incompressible flows*, SIAM J. Numer. Anal. **40** (2003), 2171–2194.
53. C. Schwab,  *$p$ - and  $hp$ -Finite element methods: Theory and applications in solid and fluid mechanics*, Oxford University Press: Numerical mathematics and scientific computation, 1998.
54. J. Schöberl, A. Arnold, J. Erb, J. M. Melenk, and T. P. Wihler, *C++11 implementation of finite elements in NGSolve*, Tech. report, Institute for Analysis and Scientific Computing, Vienna University of Technology, 2014, ASC Report 30/2014.
55. N. Sukumar and A. Tabarraei, *Conforming polygonal finite elements*, International Journal for Numerical Methods in Engineering **61** (2004), no. 12, 2045–2066.
56. A. Toselli, *hp-discontinuous Galerkin approximations for the Stokes problem*, Mathematical Models and Methods in Applied Sciences **12** (2002), no. 11, 1565–1597.
57. Q. Wang and J. Chen, *Unfitted discontinuous galerkin method for elliptic interface problems*, Journal of Applied Mathematics **13** (2014), no. 3, 1–10.
58. C. H. Wu, O. M. Faltinsen, and B. F. Chen, *Time-independent finite difference and ghost cell method to study sloshing liquid in 2d and 3d tanks with internal structures*, Comm. Comput. Phys. **13** (2013), no. 3, 780–800.
59. H. Wu and Y. Xiao, *An unfitted  $hp$ -interface penalty finite element method for elliptic interface problems*, Journal of Computational Mathematics **37** (2018), no. 3, 316–339.